POLITECNICO DI TORINO

Mechanical Engineering

A.Y. 2021/2022

Master’s Thesis

Contact pressures in internally toothed gears

Supervisor:

Prof. Carlo Rosso

Co-supervisor:

Ing. Fabio Bruzzone

Candidate:

Claudio Di Lallo

Abstract

Internally toothed gears are used in planetary gearsets, a type of mechanical power transmission with high transmission ratios and a very compact design.

The MATLAB scrip that acts as the basis for the results that have been obtained, was already capable of analysing the static transmission error, load sharing factor and contact pressures of a set of spur or helical gears. Starting from this software, the necessary modifications have been performed to achieve the same study for the meshing of an internal, or ring gear, with the planet of the epicyclic gearing. Particular attention has been aimed at correctly determining the contact pressures generated by the gear meshing. Contact pressures are of fundamental importance in determining the surface strength of gears, and even though the technical standards offer much literature to account for the different loading conditions and possible coupling between different gears, a more detailed result can lead to a better evaluation of the contact stresses, especially in the tip and root region of the tooth. To achieve these results the static loading condition of the coupling is considered, calculating the load sharing factor and static transmission error. As a final step the relative distances between the statically loaded profiles is computed, leading to the computation of the teeth profiles deformation and of the contact pressures. This approach allows to evaluate the difference between various possible tooth modifications that can enhance performance and durability of gears.

Contents

List of figures

Introduction

Motivations

The push for greater performance, and lower noise, vibration, and harshness in the transmission of power drives the demand for designing tools for gears. The manufacturing techniques that have been adopted to satisfy this demand can include the addition of many possible profile modifications. To rapidly analyse the effects of each parameter on the performance of the gears, a fast and inexpensive approach is ideal. A software can be the perfect tool for achieving these results, by rapidly computing the static, dynamic, and contact effects of the loading of gears. The host company “Gedy Trass” had already developed a model for the analysis of the main factors that affect the performance of transmissions. Given the vast field of application for epicyclical gearsets, the addition of the modelling of this type of transmission, can satisfy a broader share of the transmission manufacturing industry.

Methods

The part of script that will be studied and adapted goes from the generation of the profile of the tooth, to the evaluation of the static effects of the loading between one gear coupling. This coupling is composed of two gears, the planet gear and the annulus, or ring gear. The input for the generation of the profiles will be discussed, as well as the possible issues in the assembly of the complete epicyclic gearset, ending with the composition of the tri dimensional planetary gearset. After the coupling that includes the ring gear, and one planet can enter the script that evaluates the static loading condition of the gear, including the load sharing factor, the static transmission error, and the contact pressures. To evaluate the stresses both analytical and finite element methods will be used. The script uses the Timoshenko beam model for the deflection and a model by Sainsot, Velex and Duverger for the foundation compliance of the tooth [7]. The evaluation of the displacement of the teeth from static loading allows for the computation of the new contact point, and the contact pressures on them. This is achieved with the model in [5], and consists in the iterative computation of the displacement, that multiplied by the stiffness matrix of the surfaces, gives the contact pressures. This operation can be performed for any relative angular position between the teeth.

Epicyclic gearing

Features and advantages of the planetary gearset

In the field of mechanical power transmissions epicyclic gearset have many possible applications. The planetary gearset is composed of four main elements. The sun is at the centre, linked to a shaft the enters the whole system. The planets that mesh both with the sun and the ring gear, and whose axis are connected to the carrier. The Ring gear, that is internally toothed and meshes only with the planets. The planet carrier that connects the centre of the planet gears, keeping them in the correct position, and connecting them to the output shaft. The sun, the ring, or the carrier can be the input, output, or fixed element of the transmission. This means that if the sun is the input and the ring is the output, the carrier is the fixed element of the transmission. This does not mean that the planets do not rotate, but the carrier that holds them does not. Therefore, the power enters the transmission via the sun gear, is then split into the planet gears, and is then transmitted from the planets to the ring gear. This allows the torques to be split into multiple meshing couples. If the transmission splits the torque equally between three planets, the load that each teeth coupling is subjected to is 1/3rd of the total, allowing for the transmission of greater torques, or the reduction of the dimensions of the gears. Moreover, it is possible to have three transmission ratios, by fixing the carrier, the sun, or the ring gear.

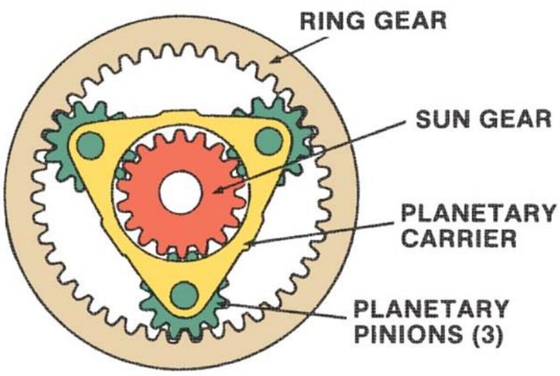

Figure 1 "Planetary gearset: main elements"

Other features that make this type of transmission appreciated are the high reduction ratios, compact and enclosed housing, co-axiality of the input and output shaft, and better performance than simple gears with the same dimensions.

Fields of application

For the abovementioned reasons epicyclical gearing has fields of application that vary greatly in dimensions, from small electric tools to massive wind turbines. One case in which this type of transmission is in competition, is the bike transmissions. The most common type of transmission for this application is the derailleur gears, that offer a light and efficient transmission of power. The other type of transmission that is used in bikes, is the in-hub type, that consists of an epicyclic transmission inside of the hub of the rear gear of the bike. This solution is adopted for utilitarian bikes, that are focused more on the reliability than on performance. The enclosed design prevents the contamination of the gearing by external elements, that can be usually encountered by a bike used daily. This can greatly reduce the maintenance of the transmission, and prevent the formation of rust from salt, or water that is picked up from the road. Another important sector in which the planetary gearset has found possible applications is the automotive industry. Automatic transmissions that use a torque converter as the launching device, can then shift between three different gears thanks to the use of planetary gearsets. This is achieved by means of clutched and brakes, that can lock either the two or more series mounted planetary gearsets. In this field, another planetary gearset has found application, the Ravigneaux gearset, that is able to produce six different transmission ratios with only one set of gears. This is achieved by having two sets of planets, and two sun gears of different dimensions. In more recent years they found another possible application in the automotive industry in the field of hybrid powertrains to couple the internal combustion engine, the electric motor, and the output shaft, that is linked both to the differential and to the electric generator. This is a particular application for parallel hybrid vehicles, that allows to greatly simplify the design, moreover, it makes it possible for the electric motor to substitute the starter motor.

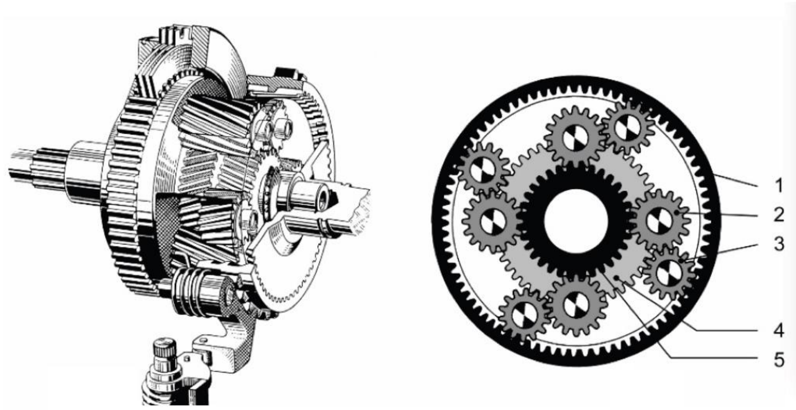

Figure 2 "Ravigneaux gearset"

Given all these possible applications; being able to simulate the manufacturing and behaviour of internally toothed gear is an important part for a software that aims at easing the design process for gears and transmissions.

Geometrical limitations

Moreover, it has been decided that the user would choose the number of teeth of the sun and the planet to define the transmission ratios of the epicyclic gearset, therefore also these parameters enter in the function that computes the combination of sun, planet, and ring, of the epicyclic gearset.

As a first step the function computes the number of teeth of the ring gear.

$$z_{ring} = 2 * z_{planet} + z_{sun}$$

If the number of planets is larger than three, some interference might occur between them, therefore a formula to check for this eventuality is added. If the size of the planet gear is too large with respect to the sun gear, the maximum number of planets that can be fitted is reduced. Given that the modulus of all the gears is the same, this leads to the conclusion that the relative difference in number of teeth between the sun and the planet is limited.

For the case with 4 planets:

$$z_{planet} < z_{sun} * \sqrt{2} - 2$$

For the case with 5 planets:

$$z_{planet} < \frac{z_{sun}}{4} * \frac{\sqrt{10 - 2 * \sqrt{5}}}{1 - \frac{\sqrt{10 - 2 * \sqrt{5}}}{4}} - 2$$

ISO check for bending fatigue

As a first step, we have evaluated the strength of the gear coupling to the bending fatigue phenomenon. To perform this analysis, we have used the BS ISO 6336-3:2019 norm. The result will be the safety factor for the ring and for the planet.

$$S_{F,Ring} = \frac{\sigma_{FG,Ring}}{\sigma_{F,Ring}}$$

$$S_{F,Planet} = \frac{\sigma_{FG,Planet}}{\sigma_{F,Planet}}$$

With σ_F tooth root stress, and σ_{FG} tooth root stress limit. To allow the computation of this value it is necessary that all the required inputs are given to the script. We have considered each coupling of gears, as its own. Therefore, the parameters that will enter the system are given as independent values, even though for a planetary gearset these parameters are related to its working condition.

Since this check was already present as its standalone function, we have checked that it worked correctly for the case of internal gears, and the eventual modifications to this script where developed. The formulas for the values that compute the safety factor can be found in the technical norm handbooks.

If the value of the safety factor is lower than one, the script returns to keyboard and asks the user if it wants to perform the calculation even though the gear coupling strength is too low for the given torque. If this condition is not respected, the following computation might give results that do not correspond to the actual behaviour of the gear coupling.

Surface strength of the tooth

The surface strength of the tooth is an important property of gears, that every gear designer should carefully check. Localized stresses and sliding between the teeth profiles, can cause a wearing of the surface. To evaluate this phenomenon, it is necessary to have knowledge of the real loading effect on the tooth, the shape of the tooth profile, and the contact stresses that arise in the loading of the gears. This process is not harmful and can occur during the run-in phase of gears. The effect of this process is a smoothing of the surface that lowers the contact stresses

Damage of the tooth surface

Pitting, as the name suggest, is the formation of small pits where once was the material. This is caused by a repeated loading that produces contact stresses above the surface strength of the material. The pitting phenomena can be divided into two subsequent processes. Initial pitting consists in the formation of small pits, and the removal of the oversized peaks of the surface roughness. If, after this smoothing action, the loads are still too high, a progressive and destructive process that removes the surface of the tooth occurs. In this process much deeper pits are formed. Once the surface has been cracked, the lubricant that is used in the gearing enters them, and the high contact pressures cause the cracks to expand. If the process continues for long enough, bigger pieces of the material will start to be removed from the tooth surface, at that point, it is possible that the pitting extends to the whole flank of the tooth. The degree of tolerance to pitting of each gear coupling depends on the field of application in which the gears will work. To prevent this phenomenon, it is important to know the surface resistance of the tooth, the contact stresses, and the sliding velocity between the meshing teeth profiles.

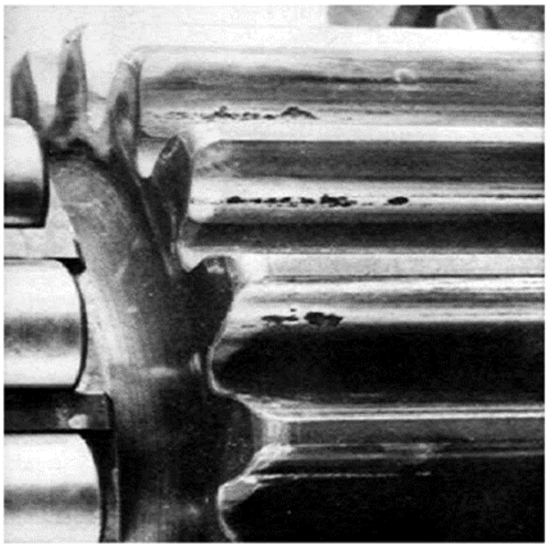

Figure 2 "Gear affected by surface pitting"

Another destructing process that affects gears is the scuffing, or scoring, of the tooth surface. Metal surfaces in contact, subjected to heavy loads, and with insufficient lubrication can undergo this severe type of adhesive wear. When there is metal to metal contact, especially in high load conditions micro-welding might occur, and some material of one surface can end up on the other surface. This metal particles that are transferred from one to the other tooth, can scratch the surface of the gears in the sliding direction. This phenomenon is primarily caused by the lack of lubrication. The lack of any type of a layer of non-adhesive material between metal is also well known to the aerospace industry. Since in space there is no air, it is possible that two metal surfaces that are in contact with a certain force, might cold weld, permanently gluing the parts together. Since the lack of lubrication is the main culprit, generally this occurs where the sliding velocities between the profiles are higher, further away from the pitch line. Another aspect that influences the lack is lubrication is the roughness of the material; gears that have not been run in, and smoothed in the process, are not lubricated as well. For this reason, scuffling especially occurs in gears that have not been run in, or has the profile grinded. Even though this process can be avoided by improving the lubrication, also the contact stresses and the sliding velocities play a role, and the computation of both will be performed by the script.

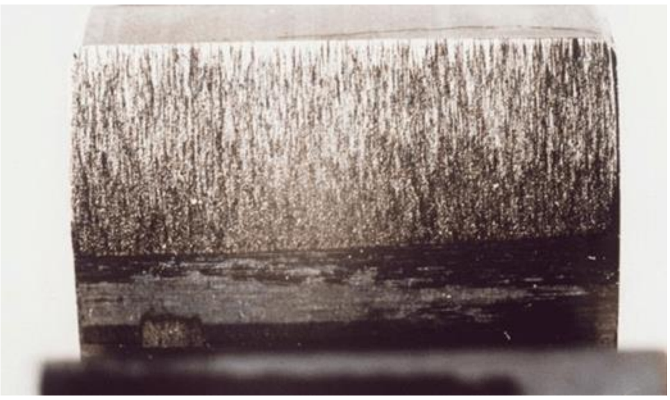

Figure 3 "Gear affected by scuffing"

Parameters that affect the computation of the pressure

The ISO 6336-2 norm was developed to verify the surface durability of gears. The application of this norm consists in the calculation of two contact stresses. This standard can provide us with the possible parameters that affect the contact mechanics, and the phenomena that influence its magnitude. The application of this norm provides the designer with the contact strength of the relevant point σ_H, that must be compared with the permissible contact strength σ_{HP}. To compute the value of σ_H, the nominal pressure at the pitch point σ_{H0} is computed as follows:

$$\sigma_{H0} = Z_H * Z_E * Z_\varepsilon * Z_\beta * \sqrt{\frac{F_t}{d_1 b}\frac{u+1}{u}}$$

This formula derives from the Hertzian contact theory for cylinders and is then corrected by the Z factors to produce the corrected result. The different approach that will be used to compute the pressures that arise from the contact between the teeth will be able to bypass the correction values and give an accurate result by studying the actual meshing condition between the teeth.

In the ISO norm, Z_H transforms the tangential load into normal load, the respective function will directly compute this value for the loading condition that is considered.

Z_E is the elasticity factor, that accounts for the specific properties of the material, such as the Young's modulus and Poisson's ratio, we will use this values directly in the computation of the pressure.

Z_ε and Z_β will be accounted for by computing the load sharing factor and generating the tri dimensional profile of the tooth.

For the computation of the pressure at the relevant point, the ISO standard provides this formula:

$$\sigma_{H1/2} = Z_{B/D} * \sigma_{H0} * \sqrt{K_A * K_\gamma * K_v * K_{H\beta} * K_{H\alpha}}$$

Currently the functions of the script can account for $Z_{B/D}$, that converts the pressures from the pitch point to the relevant point; this is not necessary since the pressures will be calculated at the exact point of contact between the profiles. Moreover, it will account for the elastic deformation of the tooth from the contact forces, that is considered in the computation of the $K_{H\beta}$ parameter. This will be achieved by computing the load sharing factor and the static transmission error. The load sharing factor is the fraction of the total load transferred by each of the teeth couples that are in contact; the static transmission error, computes the difference between the theoretical profile position, and the actual one cause by the deformation of the teeth under loading.

Currently the function can account also for the other correction factors, but only for external gears. For planetary gearsets the dynamic effects, internal and external, are not accounted for, this is cause by the loading condition of the gears in the planetary gearset. The ring gear, just like the sun, is loaded in multiple places along the circumference, depending on the total number of planets; the planets mesh at the same time with the ring gear, and the sun gear. Currently the script can consider the meshing with only another gear, therefore, the dynamic effects and the load variations on each coupling cannot be studied.

For the computation of the permissible contact stress, σ_{HB}, different possible methods are given by the standard. To understand how it is computed, and what are the factors that influence this value, we are going to describe the general formula of the method B:

$$\sigma_{HP} = \frac{\sigma_{H\,lim} * Z_{NT}}{S_{H\,min}} * Z_L * Z_V * Z_R * Z_W * Z_X = \frac{\sigma_{HG}}{S_{H\,min}}$$

$\sigma_{H\,lim}$ is the allowable stress in contact, and depends on the material strength, the heat treatment, and the surface roughness.

Z_{NT} is the life factor, if the gear has to withstand a limited number of cycles.

Z_L, Z_V, Z_R cover the influence of the oil film, respectively, oil viscosity, surface roughness, and velocity factor.

Z_W is the work hardening factor.

Z_X is the size factor.

$S_{H\,min}$ is the minimum required safety factor for surface durability.

These parameters depend on the choice of lubrication, material, and other parameters that will be decided by the designer. The phenomena that they describe concern the material and lubrication of the gears, and do not impact the computation of the contact pressures. Therefore, they are of no interest in the computation of the contact pressure.

In the following chapters we will describe how the problems in the computation of the actual contact pressures will be handled. Moreover, the script will be able to handle profile modifications. This changes in the profile of the teeth of gears, have been developed to reduce NVH in the meshing, and increase the performance by reducing the pressure peaks that might occur on certain parts of the tooth, especially near the tip, or the fillet of the tooth.

Generation of the 2D profiles

The software simulates the actual cutting process of the gear and was already fully developed for external gears. The manufacturing process that is used as a basis for the generation of the gear profiles is the rack cutting of a blank. A two-dimensional rack shape is created and simulating the movement of it, the positions are saved in the x-y plane. From this array of coordinates that are saved, the resulting shape of the gear tooth is numerically derived. This allows to directly change various parameters of the rack that affect the final shape of the gear, such as the root and tip radii, the pressure angle, shift coefficients, and any other possible rack modification.

Rack profile

The first step in the simulation of the gear cutting process consists in the generation of the cutting rack. The standard shape of the rack is very simple and is show in the adjacent figure. It is possible to modify the shape of the rack to achieve different possible tooth modifications. This is achieved in the script that defines the racks. The main modifications that can be added to the rack are the root and rip radii, the protuberance on the dedendum part, and the ramp angle on the addendum part. All these modifications are saved in the respective variables, this variable, as previously stated will enter the function that simulates the gear cutting and depending on the profile modification that is needed will alter the profile of the rack in the corresponding part. The parameters that have been used for the computation of the rack profile of the sun and planet gear, are reported in the table below. They are racks for the generation of spur gears, without any modification. It has to be noted that a small tip radius coefficient is added, in order to have a small circular fitting is added to the tip, in order to prevent a sharp edge.

Rack number	rack 1	rack 2
Pressure angle	20°	20°
Helix angle	0°	0°
Module	5 mm	5 mm
Dedendum coefficient	1	1
Addendum coefficient	1.25	1.25
Root form height coefficient	0	0

Ramp angle	0	0
Protuberance angle	0	0
Protuberance height coefficient	0	0
Root radius coefficient	0	0
Tip radius coefficient	0.001	0.001

Table 1 "Parameters of the racks that generate the sun and planet gear"

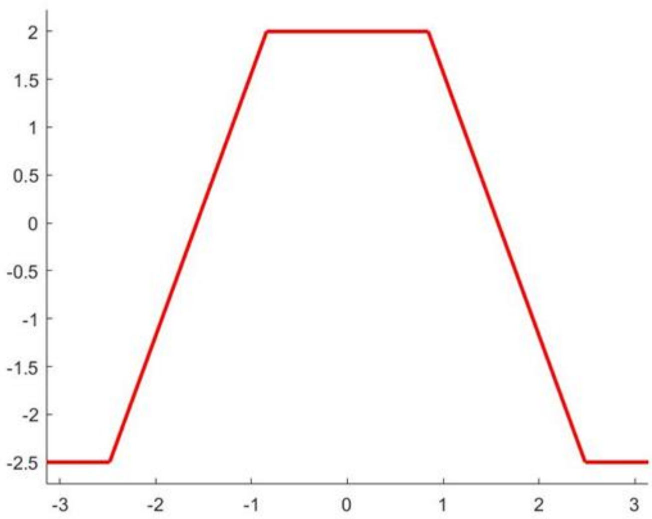

Figure 4 "Profile of the rack"

After all the parameters necessary for the definition of the rack, its shape is defined and saved in a structure that holds the segments of the rack profile in cartesian coordinates (x, y). The shape of the rack is presented in the figure 5. It can be noted that the addendum is smaller than the dedendum, since its geometry will be inverted. The dedendum becomes the addendum of the gear, and vice versa.

External Gear generation

The parameters for the definition of the gear that will be cut, occurs before the definition of the rack, they are, the number of teeth, the normal modulus, the teeth and body face width, the normal pressure angle, the helix angle, the rim depth, the radius of the shaft to which it is coupled, the shift coefficient, the addendum and dedendum. Moreover, it is possible to add some other profiles modification, like crowning, tip relief, root relief, and other. The parameters of the case that has been studied are reported in the following table, together with some other parameters used to generate the 3D shape of the gears.

Gear	Sun	Planet
Number of teeth	24	33
Modulus	5 mm	5 mm

Face width	40 mm	40 mm
Gear body face width	40 mm	40 mm
Pressure angle	20°	20°
Helix angle	0°	0°
Rim depth	5 mm	5 mm
External radius of the shaft	40 mm	55 mm
Shift coefficient	0	0
Addendum	1	1
Dedendum	1.25	1.25
Backlash	$0\ \mu m$	$0\ \mu m$
Crowning	None	None
Tip relief	None	None
Root relief	None	None

Table 2 "Parameters of the sun and planet gears"

Going back to the function that generates the profile of the tooth, after the rack shape has been determined, the script will simulate the actual cutting process of the tooth. This happens by computing the position of the rack with respect to the gear blank. Once the rack relative motion has been completed, the profile of the internal tooth is extrapolated and saved both as cartesian, and as polar coordinates. In the figure below the results of the movement of the rack are plotted with the black lines, and the final profile of the tooth is in blue. The generation was performed correctly, and as can be seen, the unshifted pitch line is at 60 mm, that is equal to the number of teeth multiplied by the module and divided by to. From the pitch line, the tip lays 5 mm above, since the addendum coefficient is one, and the dedendum circle is 7.5 mm below, given the dedendum coefficient of 1.25.

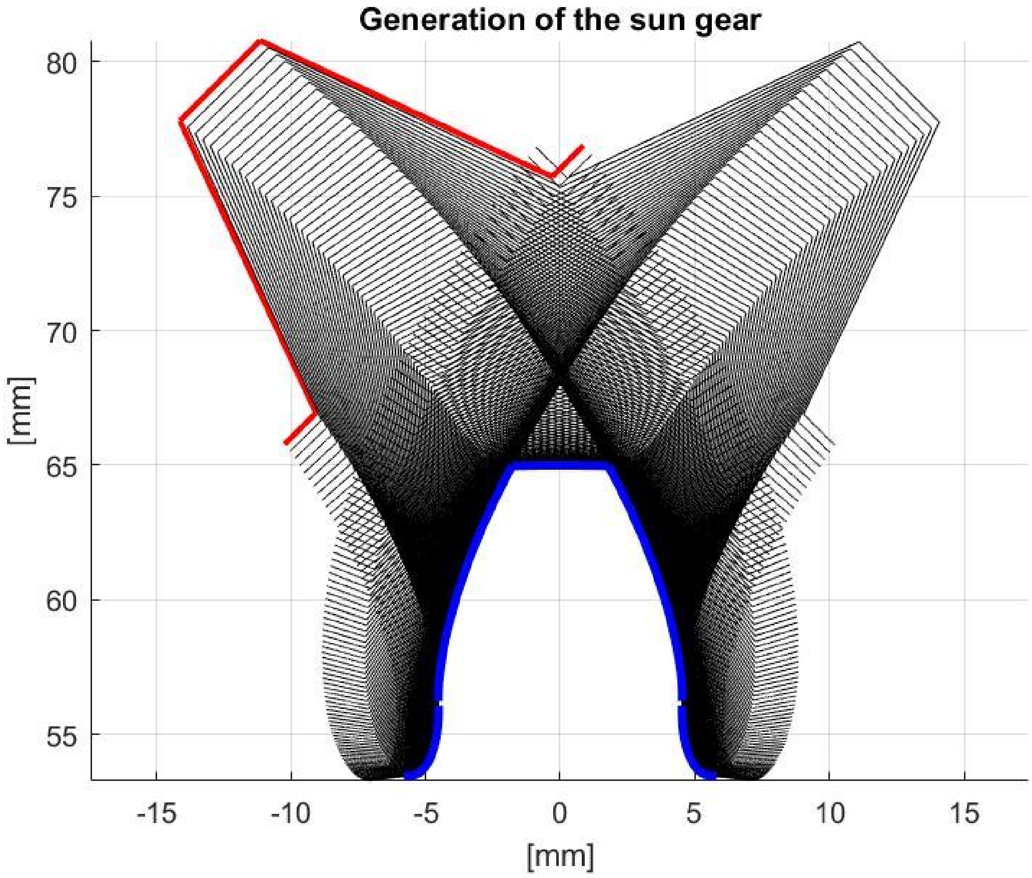

Figure 5 "Simulation of the cutting process of the sun gear"

Internal gears generation

The manufacturing process for internal gears is different from the one of the externals. The two main processes for the blank cutting of the annulus are performed either by a shaper gear or by a broach. The script has been developed as to simulate the cutting process by a shaper gear. Therefore, the first step in deriving the points of the profile of the ring gear is to correctly generate a shaper gear that will perform the cutting. This process is not much different from the generation of an external gear, the most important parts are the correct definition of the addendum and dedendum of the rack, that will be inverted, and correctly sizing the number of teeth of the shaper gear. If the ring gear has a standard addendum $h_a = 1$ and dedendum $h_d = 1.25$, then the shaper gear that will form it, must have the values inverted, $h_d = 1$ and $h_a = 1.25$, since the profile of it will become the vane of the internal gear. For sizing the shaper gear a general value of 1/3rd the size of the annulus has been used. This usually grants a good cutting process, and prevents unwarranted interferences, that will be analysed in the next chapter. Once the shaper profile has been determined, and it has been saved, the script proceeds with the generation of the internal gear. In the first version the shaper was modified, and a root fillet added, but since the addition of this root fillet would cause an addition of material on the tip of the internal gear, it has been discarded. This decision has been taken because the tip of the internal gear would have interfered with the root of the teeth of the planet gear, that's because the removal of material from the shaper leads to an addition of material on the internal tooth profile. Another important parameter that has been modified for the ring gear, is the external radius of the shaft, that for internally toothed gear is used to plot the external rim of the gear, therefore, it is larger than the pitch radius of the gear. Moreover, the possibility of adding the backlash to the ring gear was added, and to check that the feature works correctly a 100 μm backlash has been added.

	Rack of the shaper	Shaper	Ring gear
Number of teeth	-	30	90
Modulus	5 mm	5 mm	5 mm
Face width	-	-	40mm
Gear body face width	-	-	40mm
Pressure angle	20°	20°	20°
Helix angle	0°	0°	0°
Rim depth	-	-	5 mm
External radius of the shaft	-	-	270 mm
Shift coefficient	0	0	0
Addendum	1	1.25	1
Dedendum	1.25	1	1.25
Backlash	-	-	100 μm

Table 3 "Parameters necessary for the generation of the ring gear"

Interference between the planet and the annulus

The issue of interference for the meshing of internal gears is quite complex and can be divided in five main types. Only the first one has been added to the script, since it is the one that can be easily calculated, with an analytical formula. In the other cases, the check can be performed by means of tables and graphs. Since the use of a software would not add insight or reduce the time to compute these types of interference it has not been added. For the case that will be studied we have checked that no interference occurred between the planet and the ring gear.

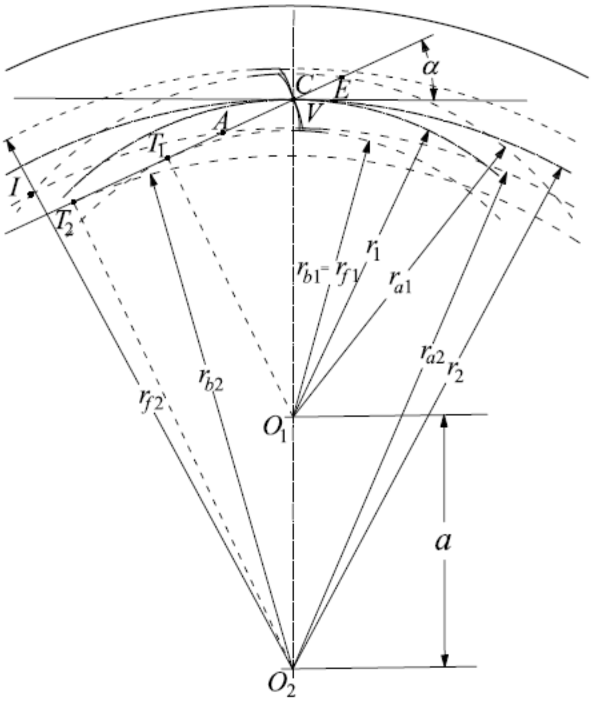

Figure 6 "Design parameters of the meshing between internally and externally toothed gears"

Theoretical interference in the internal spur gear

This type is the same as the one in external gears and happens if the path of contact goes beyond the points T_1 or T_2 defined as the points perpendicular to the base circle.

It is possible to check for this type of interference simply by making sure that the following inequality is satisfied:

$$r_{a2} \geq \overline{O_2T_1} = \sqrt{\overline{O_2T_2}^2 + \overline{T_1T_2}^2} = \sqrt{r_{b2}^2 + [(r_2 - r_1)\sin\alpha]^2}$$

The values with subscript 2 refer to the ring gear, and the one with subscript 1, to the planet gear, the radii and the points are also represented in figure 7.

In the case that this type of interference occurs it is possible to use nonstandard addendum coefficients. This practice is quite common in the design of internally toothed gears, that might have the addendum that is lower than the module of the gear. The script that checks for this type of interference has been implemented, and if the combination of gears that has been selected features this type of interference an error message will be displayed, asking the user if he wants to continue with the following computations.

Secondary interference in internally toothed gears

Secondary interference, also called fouling, only occurs if the pinion size is close to the size of the internal gear. This phenomenon occurs outside of the path of contact between the internally and externally toothed gears. In the region represented in the figure below, it is possible that the tooth of the planet gear might notch the tooth of the ring gear in the near its tip.

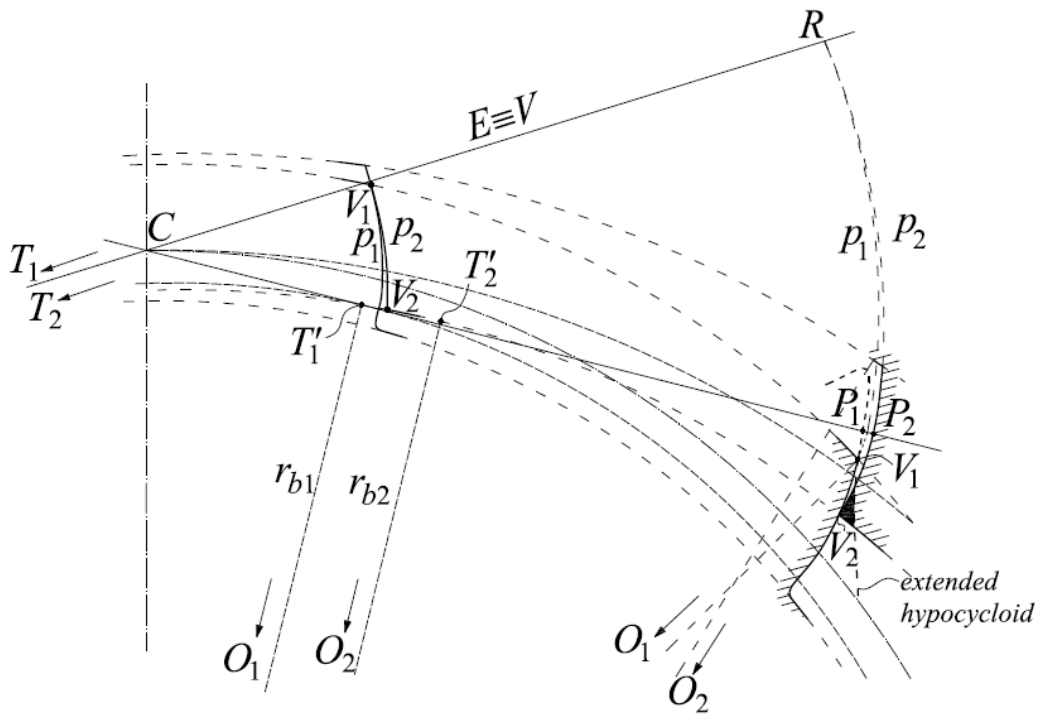

Figure 7 "Secondary interference mechanism"

To check for this type of interference it is easiest to use the tables that have been derived by Henriot shown below, that requires only to know the number of teeth of the gears, the addendum factor, and the pressure angle.

$$k_2 = k_1 = k = \frac{h_a}{m} = 1$$

With h_a addendum, and m, modulus. The case in study is the standard condition, therefore, the addendum factor is one, but it can be reduced to prevent this type of interference. This type of gearing is called stubbed because it appears that the tooth has been cut at a certain height.

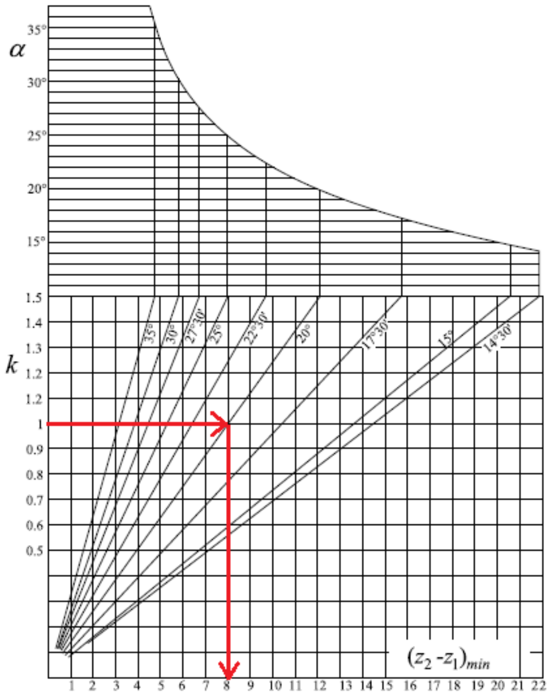

Figure 8 "Minimum difference to avoid secondary interference"

As it is possible to see from the figure above, secondary interference is not a problem in the case that has been studied, since the internal gear has ninety teeth, and the planet only thirty-three teeth. Hence the difference is of fifty-seven teeth between the two gears, a value much larger than the required eight.

Tertiary interference in the cutting process

The tertiary interference or trimming is a type of interference that might occur when cutting the gear with a pinion-type cutter. Since this is the process that will be simulated in the generation of the ring gear, it is important to check that it does not occur. This phenomenon causes a removal of the flank material towards the addendum line, preventing the radial assembly of the gearset. The derivation of the possible condition of interference is quite complex, and it ends with the conclusion that the difference in number of teeth between the ring gear and the shaper or pinion-type cutter must be larger than the one evaluated in the secondary interference. To avoid a very complex study, that requires many steps, Heriot proposes a simple rule, the difference in number of teeth determined for the secondary interference must be increased by six.

$$(z_{ring} - z_{shaper})_{min} > (z_{ring} - z_{planet})_{min} + 6$$

From the previous computation it is therefore necessary that the difference is greater than fourteen. Since in our case the shaper has thirty teeth, and the ring gear ninety, the difference, of sixty teeth is more than sufficient to avoid this type of interference.

Fillet interferences between the tips and the roots

The last two types of interference that might occur between the planet and the ring gear are between the tip of the pinion and the root of the annulus, and between the tip of the annulus and the root of the planet gear.

The formula to check for this type of interference has not been developed, but the meshing profiles have been manually checked, and it has been determined that this type of interference is not present in the case in study.

From the shaper profile to the internal gear profile

Before the actual simulation of the cutting process of the internal gear, the possibility of adding the backlash to the annulus has been implemented. The substantial difference lays in the fact that to add the backlash there must be an alteration of the movement of the shaper gear, and not of the rack. Therefore, the necessary lines that make it possible to alter the tool movement have been added before the function that simulates the cutting process. This consists in the shifting of the pitch line for the pinion-type cutter, making it cut deeper into the blank of the ring gear.

As a first step the function must obtain the profile of the shaper gear and save it to use it in the cutting process of the ring gear. This process is very similar to the generation of a standard gear, but, as it is possible to see in table 3, the addendum and dedendum are inverted. As it will be possible the reversal of addendum and dedendum generates a profile that is quite peculiar. In the fillet region the tooth is thicker than an external gear with similar number of teeth, and pressure angle. In the tip region the profile extends more, and the tip is thinner. To obtain this geometry also the addendum and dedendum of the rack that generates it must be inverted from the standard case, as is reported in table 3.

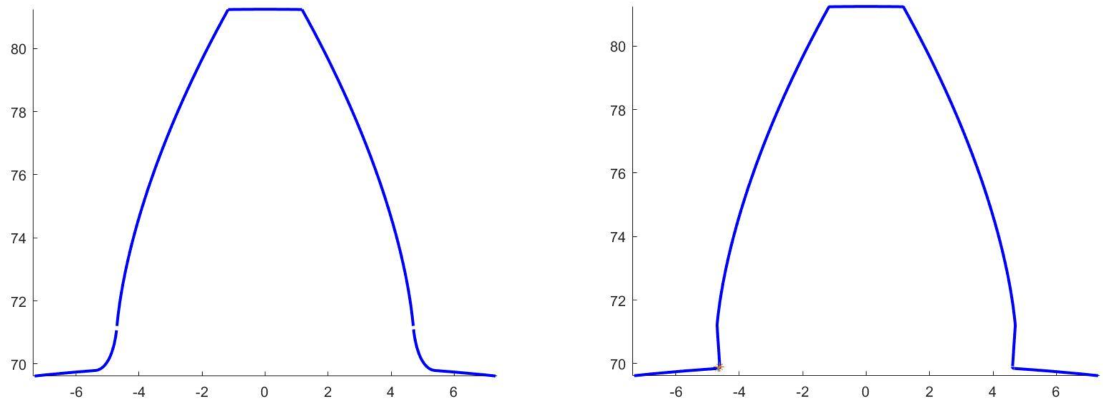

Figure 9 "Profiles of the shaper cutter, without and with the fillet fitting"

Another modification that was required, was made on the profile of the shaper gear. In the generation of the shaper gear, after the cutting process from the rack ended, a fillet radius at the base of the tooth of the shaper was added. This modification, as it can be seen in the figure 10b, removed some material at the base of the tooth. The removal of this material caused the shaper gear to limit the cutting of the ring gear towards the tip, leading to the formation of a protuberance on the. Even though this process might be possible in the manufacturing of the shaper gear for the cutting of internally toothed gears, it leads to an interference problem when the ring gear meshes with the planet.

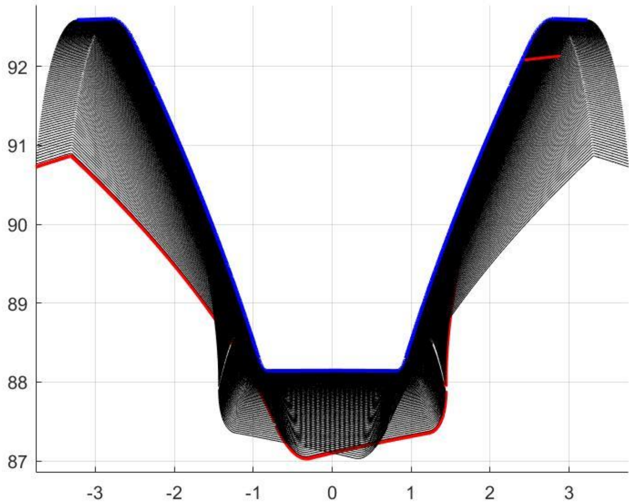

Figure 10"Generation of the ring gear"

As it can be seen in the figure, if the shaper, that is in red, had the shape that was previously generated, it would remove less material on the internal gear blank, generating the abovementioned protuberance. This protuberance would go into contact with the lower part of the flank of the planet gears, causing an uneven motion between the two gears, since this part would not be an involute profile. For this reason, we removed the circular fitting, and kept the rest of the work that was previously done on the generation of the profile of internally toothed gears. The profile of ring gear is then saved in the same way as other gears, in two structures that contain respectively the cartesian and polar coordinates of the points of the profile.

Tooth profile definition

The data that has been derived from the simulated cutting process of the gear must be manipulated to pass from the structures that contain the data of the profile, to a tri dimensional profile that is separated into root, fillet, flank, and tip. This process will be performed for each of the two flanks of the gear, making it possible to simulate a clockwise or counterclockwise rotation between the gears. The right flank of the gear is defined when looking at the side profile of top tooth of the gear.

The flank of the tooth profile

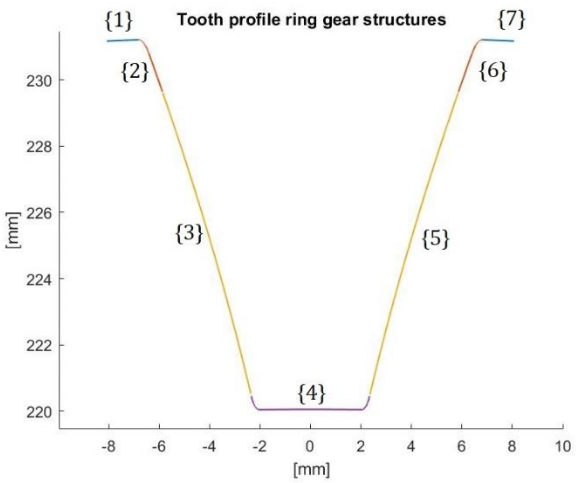

Figure 11 "Segments of the tooth profile"

The two-dimensional shapes that have been previously generated will form the basis for the computation of the (x, y, z) coordinates of the surfaces of the tooths. Although, since not all the tooth profile goes into contact with the other gear, it is necessary to firstly identify the flank and fillet of the gear, from the previously generated arrays. The dedicated function had to be reworked for the case of internal gears, because the position of the respective parts of the tooth is different in the structure that contains the arrays of the generated profile of the tooth. The different parts of the structures are shown in figure 12. The structures 3 and 5, that should describe the flank of the tooth, are not extended long enough. In the case of externally toothed gears, unless some profile modification has been added, there is a sharp corner between the flank and the tip. In this case, instead, there is a smooth transition from between the two elements of the tooth. This causes the script to have issues in the correct definition of each element. It is then necessary to operate differently for the ring gear. As already shown in figure 12, the script receives the coordinates of the tooth profile as a structure divided in seven arrays. The array that defines the flank is saved as the flank, and then both a part of the array that usually saves the tip and the fillet have been added to the flank. To achieve this, the lowest node of the tip array, has been considered as a base point. Its radial coordinate is increased by 1/50th of the modulus of the gear, and all the points of its structure that were above this threshold value, were moved into the flank array. The same process has been adopted to move some points of the fillet, to the flank. For this case, the maximum value of the fillet array has been decreased by 1/6th the modulus of the gear. To keep track of this modification, the new upper and lower values of the flank are saved to flag all the points that originally were not part of the flank structure as a sort of profile modification.

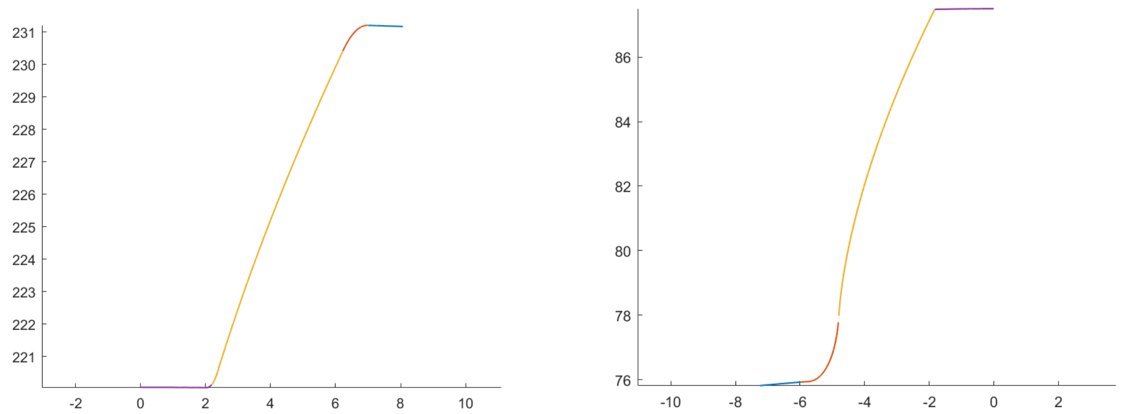

Figure 12 "Final profile of the left side of the ring and planet gear"

As it can be seen in figure 13, the profile of the tooth has been divided into the root, in blue, the fillet in red, the flank in yellow, and the tip in purple. It can also be noted that the geometry of the internal gear is inverted. The tip of the internal gear is the lowest part of the profile, whereas the tip of the planet gear is on top. The two sides of the tooth profile are saved in two distinct structures, that we will refer to from now on as right and left. This distinction is performed to ease the computation of the distances between the two flanks, since each side of the internal gear will only go in contact with the respective side of the planet gear. For example, if the direction of rotation of the system is counterclockwise and the power is transmitted from the ring gear to the planets, then the left side of the internal gear will contact the right side of the planet gear. Therefore, when computing the distance between the profile, the relevant distance is the one between these two sides of the profile. Removing the side that does not go into contact can prevent possible mistakes in the computation of this distance. An important note that is fundamental for the user, is that the script that performs this operation is a new one, distinct from the one for external gears, and it is important that the ring gear enters this function as the gear2 input, and the planet enters as the gear1 input. If this requirement is not satisfied the function will not work correctly, since it assumes that the second gear to enter as the input is the annulus.

Flank nodes and tooth profile modifications

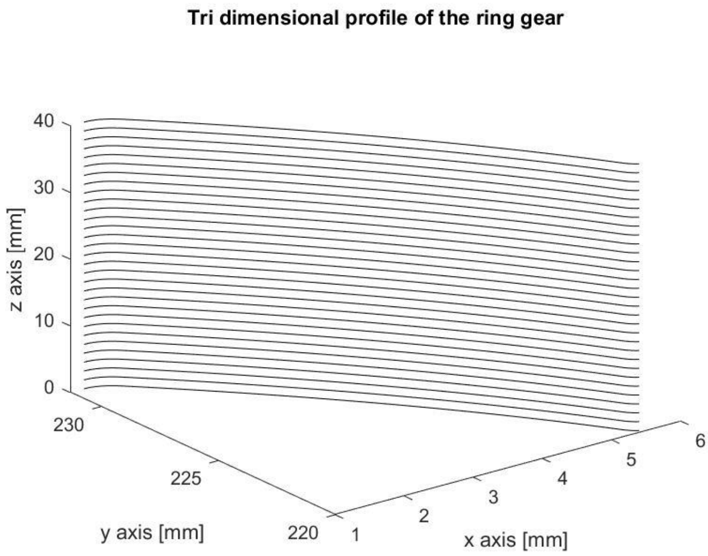

Figure 13 "3D of the flank, divided in slices"

This function takes the profile of the tooth that has been described in the previous chapter, checks its accuracy, and replicates it in thirty-one further points along the width of the tooth, thus generating the tri dimensional profile. In the case of spur gears this consist just in the copying of the x, y data of the profile on all the other z coordinates, but if helical gears are considered it must add the helix angle. As it can be seen in figure 14, the tooth width is added, by copying flank profile into thirty-one slices.

Another task of this function consists in the flagging of the part of flank that was affected by a tooth profile modification. As previously mentioned, the flank profile of the internal gear has been extended, and since there the concavity of the profile along the flank is not homogenous, the convex parts will be described as a tooth profile modification. In this part of the script the matrix that identifies if the profile has been modified is generated, and therefore the case for internal gears has been added. Using the previously saved values of the flank, all points that are below the lowest point, and above of the highest point will be flagged as a tooth profile modification, in the *moda* matrix. Not all the points that have been considered for the generation of the *moda* matrix will be in contact during the meshing of the gears. Those points will be removed both from the strings that will be used to compute the contact points, and from the respective *moda* matrix that flagged them as being part or not of a profile modification. In the standard case, it simply assumes that these points are in the lower part of the tooth, but for internally toothed gears, since the geometry is reversed, also this process must be reversed. For this reason, the opportune modifications have been added. For this function it is also important that the ring gear is the gear2 in the input, since, to limit the modifications to the script, the check for the internally toothed gears is performed only for this gear.

The teeth in contact

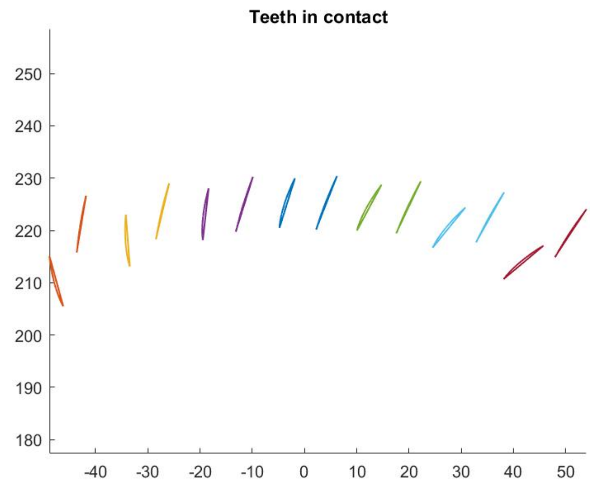

Figure 14 "Teeth that might enter contact"

Once the tri dimensional discrete model of the tooth has been realized, it is necessary to represent all the teeth that will be in contact. Instead of saving all the teeth of the gear, in its own structure, only the teeth that might get in contact have to be stored in memory. The function takes one flank profile of the tooth, makes a copy, and positions it rotated by the angular pitch distance, repeating this process for as many times as the estimated number meshing teeth. Once the process is completed, the profiles are saved in the respective structure, that will be used for the calculation of the first contact position, and of the relative distance between the profiles. As it is shown in figure 15, each colour corresponds to the tooth number of the profile plotted. Starting from the right, the 1st one is in light blue, and is the rightmost tooth both for the ring and the pinion, moving to the left, the number of the teeth coupling increases, up to 7 for the case that is presented in figure. In the next step, the profiles of the ring gear will be rotated to the left, and each profile will be positioned facing the correct tooth profile of the planet gear. To accommodate the function also for internal gears it was simply required to change the sign of the flank input. This parameter is a flag that describes which flank of the gear must be considered in the function and affects the way in which the selected teeth are numbered. As previously mentioned, the tooth number indicates to what meshing couple it belongs, therefore the tooth number one in the pinon should face the tooth with the same number in the gear. For external gears this means that the gear number is determined by considered it rotated by 180°, with the selected teeth on the bottom and facing the pinion one that are positioned on the top. For the internally toothed gear, no rotation is required for the meshing of the tooth, therefore the teeth should be numbered in the opposite order as the external case, leading to the flank flag being of opposite sing. By switching this flag when manipulating the ring gear, it is not necessary to modify the script developed for externally toothed gears.

First contact position

To correctly enter the coupling analysis, the teeth profiles must be positioned in contact with each other. The function that achieves this goal had to be modified to achieve this result. This function takes the profiles constructed in the previous function and calculates the angular distance between them. The profiles are then rotated by the angle of the closest couple of teeth. This saves the profiles of the teeth in the position of first contact. In the previous function the profiles were correctly numbered, although, the relative positions are different from the external tooth case. In fact, they are moved by half of the pitch distance in the opposite direction. In that part of the software the generation of the profiles puts the centreline of the tooth in correspondence of the y axis, and it is a good strategy for position the externally toothed gears. But since the selected teeth of ring gear are not rotated by 180° to get in the meshing condition with the other gear of the coupling, they are shifted in this way. To put the profiles of the annulus in the position that faces the corresponding profile of the planet gear, the initial rotation must be performed in the opposite direction to the standard case, the amount of the rotation is equal to 0.55 of the pitch distance. The same logic must be applied when the final rotation is performed, including the tolerance angle that is added to slightly separate the profiles. In figure 16, it is possible to see the profiles in contact; in black is the internal gear, and in red is the planet, the contact point is in the lower part of the flank for the planet, and in the upper part for the internal gear.

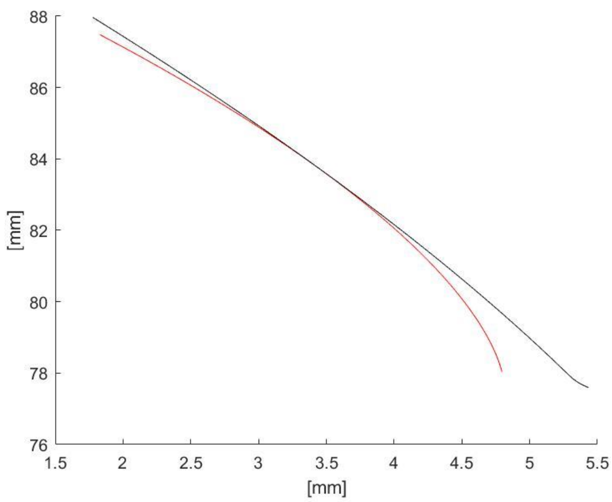

Figure 15 "Teeth in contact"

Once the angle that separates them has been determined, it is important that script rotates the profile of the internal gear, and not that of the planet gear. Since we are rotating the gears that compose a planetary gearset, it is important to think about the final assembly of the whole gearset. The script had previously performed the same operation that we are describing for this couple of gears, for the sun and the planet gears. In that instance the sun was rotated with respect to the planet gear, therefore the planet is still in the position in which it was generated. Instead of rotating the planet to the position of first contact with the annulus, if we rotated the latter, all three of the gears that compose the gearset, will be in the correct angular position. This means that, at least for the sun, the ring, and the first planet, no rotation will be required to assemble the gearset in the 3D model.

After all the operation that have been performed in this chapter are completed the relevant data will be saved in the coupling1 structure, that will enter the coupling analysis function. Although before this step is performed a compete 3D assembly of the system is generated.

Complete assembly

Three-dimensional finite element model

Once the full definition of the tooth has been achieved the whole gear can be generated as a set of polygons. A function was already developed for this task, although given the different geometry of the internal gear, it was necessary to adopt some changes. To create the polygons, both the main function that generates the inputs, and the subfunction that handles the generation of the single pieces were modified to work also with internal gears. Moreover, an improvement to the sampling of the fillet points was added; instead of picking nodes that are equally spaced in the array of all the nodes, it was changed to equally spacing the nodes in the y coordinates.

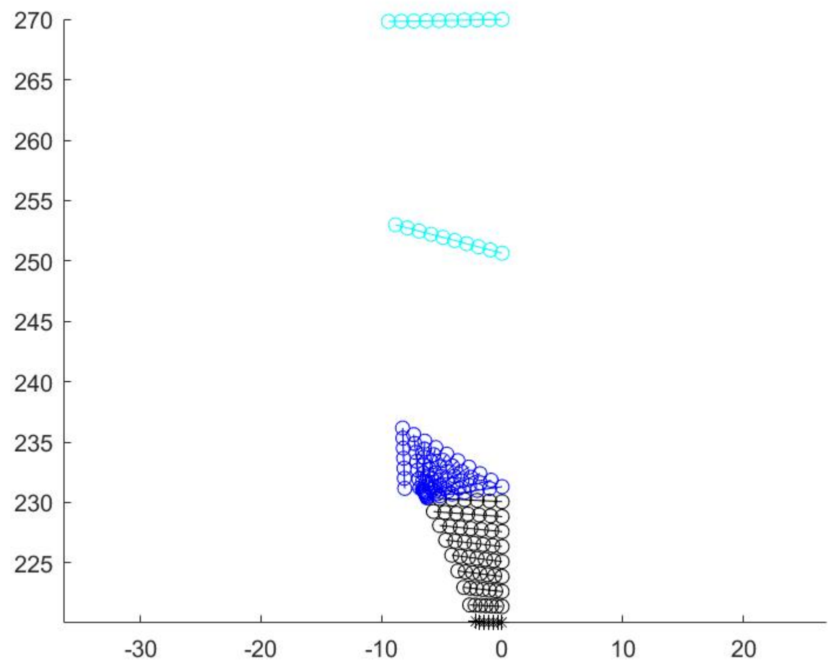

Figure 16 "Discretization for 3D model"

In figure 17 the frontal perspective of the points of discretization is shown, with 4 distinct types. On the bottom are represented with the black star the points of the tip, it is important that their number is equal to the longitudinal points of discretization of the flank, represented by the black circles. Above them lays the fillet and root points, the blue circles, that are linked to the points that join the centreline of the tooth with the centre of the root. Lastly, the light blue circles complete the mesh, by going up to the external dimensions of the ring gear.

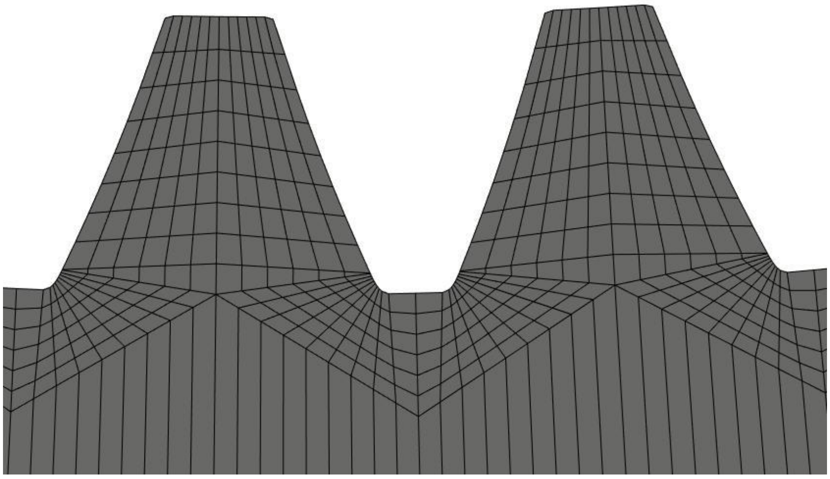

Figure 17 "Detail of FE discretization of the ring gear"

As it is possible to see in figure 18, the script correctly discretizes the ring gear. The modifications required consisted mainly in switching the angles of rotation and inverting the order of some arrays of points. Moreover, the spacing of the points of the fillet were optimized and increased to prevent the generation of triangles. It is important to check for any triangles, that might occur if not enough nodes are used to discretize a certain part of the tooth. This is relevant because this parametrization can be exported for in software for the FEM analysis of the stresses, and that software might not accept it as a correct shape, filling the gear with voids.

Once the discretization of the ring gear was successful, the whole planetary set can be plotted. Having previously accounted for the assembly of the whole set, has allowed to easily put in the correct position all the gears. The sun gear and the first planet are positioned first, without any necessary modification. Then, the latter is copied, and rotated around the sun; this is achieved with two rotations. The first is around the sun and depends on the number of planets (120° in our case with three planets).

$$\vartheta_1 = \frac{360°}{n° \; of \; planets}$$

The second time it must be rotated around its centre by the number of teeth of the sun that correspond to the first rotation:

$$\vartheta_2[deg] = \frac{\vartheta_1}{360°} * z_1 * \varphi_2$$

With z_1 number of teeth of the sun gear, and φ_2 angular pitch of the planet gear.

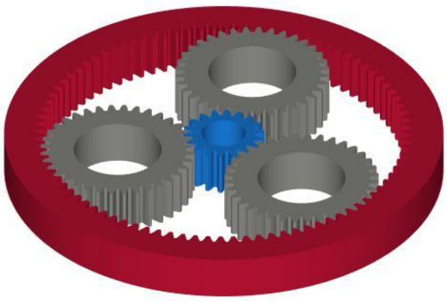

Figure 18 "3D model of the planetary gearset"

At the end it is possible to simply add the 3D model of the ring gear to the assembly, and it will correctly fit with all the planet gears, assuming that there was not a previous error message that warns the user that the combination of gears cannot fit in a gearset with the requested parameters.

Quasi-static analysis

Structure of the coupling analysis

This chapter is dedicated to the determination of the static transmission error, the load sharing factor, and the contact pressures during the meshing of the planet gear with the ring gear. The transmission error is the angular difference between the theoretical position of the gear tooth, and the actual one. This phenomenon occurs during the meshing of gears, because of the teeth deformation under loading, and from manufacturing errors of the shape of the gears. The magnitude of the transmission error is usually computed experimentally, by loading the gears with different torques at different speeds and measuring the angular position of the two. It is an important parameter when designing gears because it causes noise, vibrations, and general harshness in the transmission of the power between gears. Tooth profile modifications, in the design stage of the transmission, can greatly reduce this problem, improving the performance, and reducing noise and vibration levels. In our case we will compute only the static transmission error since the dynamic effects are not included. The value of the static transmission error varies during the meshing of the teeth, depending on how many teeth are meshing, and at what height of the tooth the force is exchanged.

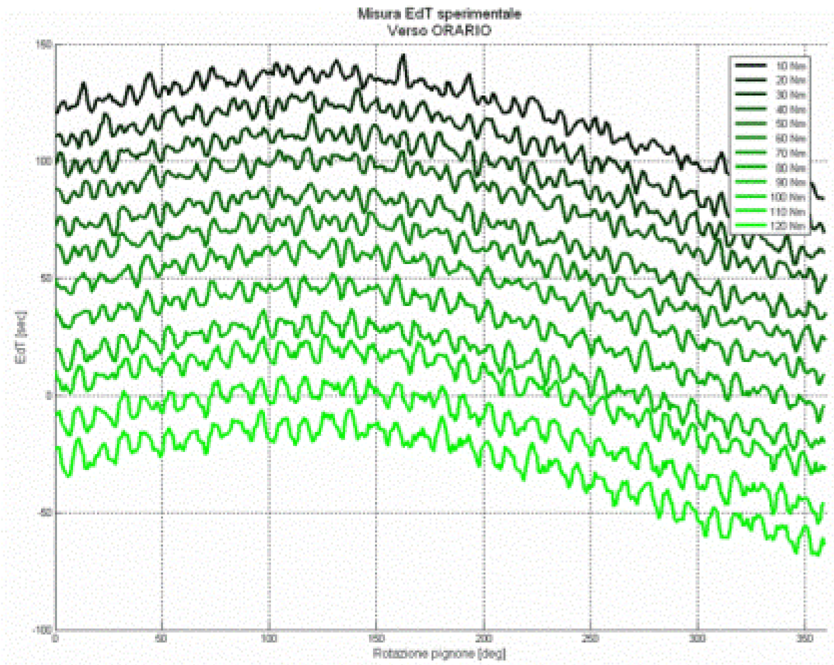

Figure 19 "Experimentally derived values of the transmission error"

To estimate the value of the static transmission error it is necessary to know the deformation and the loading of each teeth couple that is transmitting power. Since there is no closed solution of this problem, an iterative approach has been adopter. The deformation under bending is computed by means of the Timoshenko beam model, and the tooth fillet compliance will be determined with an analytical formula in reference [7]. For the computation of the load sharing factor, a more simple but effective approach is used, that will be described in detail in the relative paragraph. These values will be computed for all the positions in the loop of the angular position.

The script that handles all the further steps was developed for externally toothed gears, therefore, only one couple of gears can enter at a time. Since the focus of the study lays mainly on contact pressures, it has simply been adapted to study the mating condition between one planet gear with the ring gear, and with the sun gear. Further development of the script, that will be able to handle the mating condition between one ring gear and many planet gears has still not been developed. The two possible cases have been saved in two separate structures that contain all the necessary data computed in the previous steps.

Since the planet gear is the pinion in this coupling, to avoid mistakes, the frame of reference of the profiles that will undergo the rotations and deformations is changed. Up until now the centre of the sun gear was the centre of the frame of reference, but in our coupling 1, that enters the coupling analysis, it has been moved to the centre of the planet gear.

Below it is represented in schematic form the two main loops that compose the script for the Quasi static analysis. The j loop is for finding the equilibrium position, and the k loop for the angular positions.

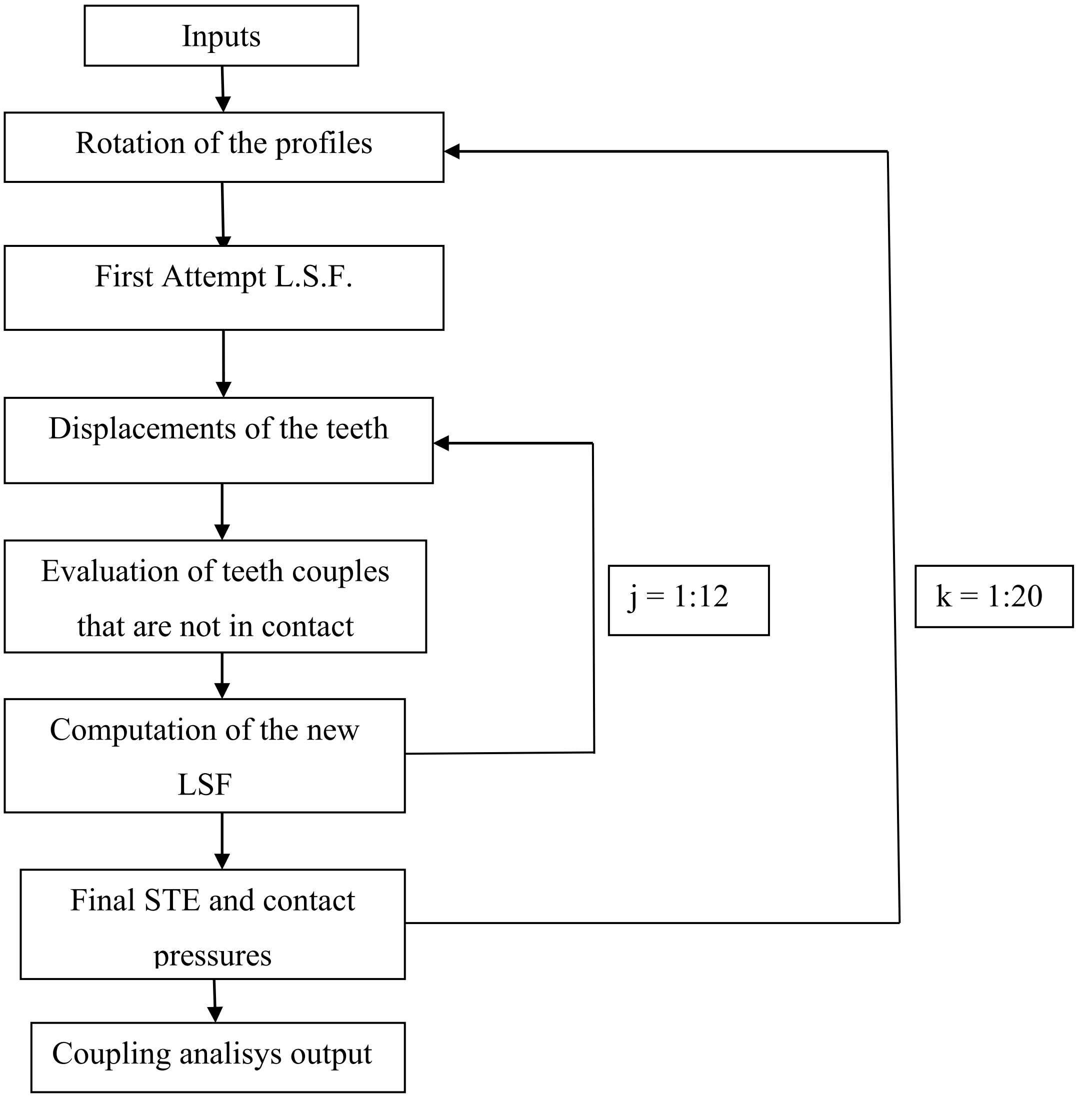

Loop of the angular positions

As it was previously mentioned, the loading point on the flank of the tooth affects all the outputs of interest. To fully understand the behaviour of the mating gears it is necessary to study more than just one loading case. Therefore, the computation of the static transmission error, load sharing factor, and contact pressures will be performed for twenty possible mating conditions, this is a compromise value that allows to study a spectrum of possible loading conditions without extending too much the computation time of the software. The angle of rotation of the tooth profiles for each step is computed by dividing the pitch angle of the pinion by the number of positions that will be studied.

$$\alpha_{rot} = \frac{360°}{z_{gear} * 20}$$

Once the profiles are correctly rotated to one of the twenty positions a first estimation of the number of teeth in contact will be performed, and the distance between each couple of meshing teeth will be computed.

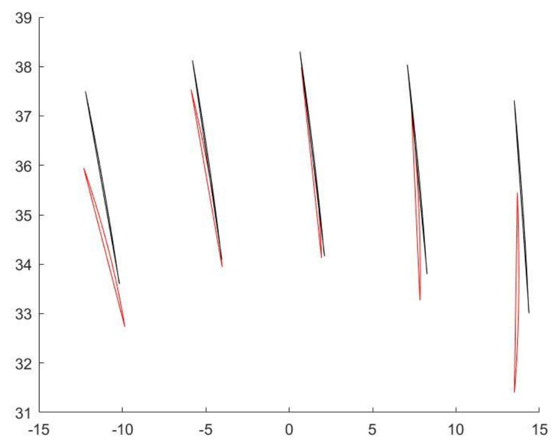

Figure 20"Profiles of the teeth for the first angular position"

If the profiles are within a certain distance they will be assumed to be in contact, and the script will return the contact node and coordinates.

Moving along the positions that will be studied, the teeth profiles rotate, and the principal couple in contact might change. When this occurs, it is necessary to switch the teeth in contact. The script will automatically perform this operation, adding one to the value of n_{st}. This will make the script enter the function that deletes the last couple of teeth, both in the pinion and in the gear, and adds a new couple on the other side. Theoretically this process could be repeated as many times as the user wishes, but since the script only considers one pitch distance, this process usually happens only once. If the script is studying the case of the internal gear, then it is necessary to change the value of n_{st} to correctly compute the distance between the profiles, and the contact point determined. This is necessary because the script was developed for external gears. In the unmodified script, if the pinion is rotating clockwise, the tooth would be added on the left side, and on the right one for the gear. In the case of an internal gear, if the tooth profile is added on the right, then it must be added in the same direction for the pinion, because of the already mentioned geometry of the gears, that does not require the 180° rotation of the gear.

Tooth stiffness matrix

Using the Timoshenko cantilever beam approach, the script can compute the stiffness matrix of the tooth with the finite element method. The flank and fillet of the tooth enter the function as the input. They are then rotated by a negative angle of 90°. This movement positions the tooth centreline coaxial with the x axis. The script then computes the section area of the tooth, and the moments of inertia around the three axes, giving the torsional moment of inertia with respect to the x axis, and the flexural moment of inertia around the y and z axes. In the case of the ring gear, the same rotation that is performed for the planet puts the tooth centreline on the x axis, but it would constrain the tip of the tooth, and not the root. To position the node that must be constrained on the left, it is therefore necessary to rotate and translate the tooth profile. To correctly position the profile of the annulus starting from the {x} and {y} coordinates of the profile, as they were computed in the first angular position, the following operations were performed:

$$\begin{cases} \{x\}_s = -\{y\} + 2 * \min\{y\} \\ \{y\}_s = \{x\} \end{cases}$$

It was decided to change this part of the script instead of producing a different stiffness matrix of the tooth, because there is practically no difference in the computation time of the rotation and translation, compared with only the rotation. The generation of another script for the computation of the stiffness matrix would have been completely redundant since the difference lays only in the constraining of the node.

After the profiles are positioned correctly it is possible to compute the entries of the stiffness matrix. The shear modulus and the shear factor for the Timoshenko beam for the material are computed as following:

$$G_1 = \frac{E}{2(1+\nu)}$$

$$k_b = \frac{10(1+\nu)}{(12+11\nu)}$$

With E Young's modulus, and ν Poisson's coefficient of the material. Then the area, A, the moments of inertia I_y and I_z, are computed in the following way:

$$A_j = y_{s,j} * b$$

$$I_{y,j} = \frac{b^3 * y_{s,j}}{12}$$

$$I_{z,j} = \frac{b * y_{s,j}^3}{12}$$

Once all the necessary parameters have been derived, it is possible to generate the stiffness matrix of the tooth, including the distance between the nodes in the x-axis:

$$\delta_{s,j} = x_{s,j+1} - x_{s,j}$$

Since the stiffness matrix size is very large and would require too much memory to be saved as a full matrix, it is then saved as a sparse matrix, and inverted, giving the compliance matrix, that is the final output of the function.

In the figures below the various values for the section area, and moment of inertia of the ring gear are represented.

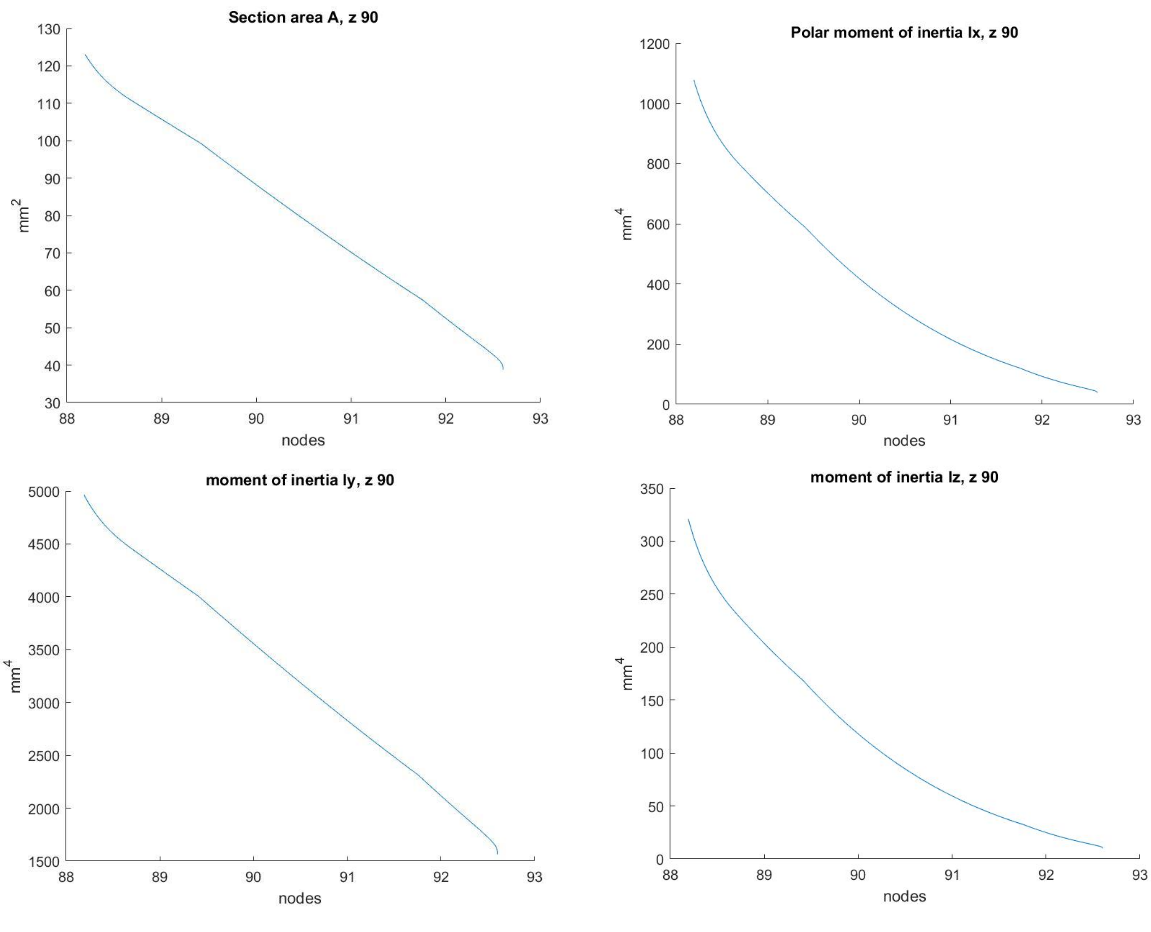

Figure 21"Geometric parameters of the tooth of the ring gear"

The stiffness matrix that has been constructed in this step will make it possible to compute the deflection of the tooth, and it can be computed once, before the loop of the angular positions, since it does not depend on the angular position of the tooth.

Contact plane construction

The previous part makes it possible to compute the bending resistance of the tooth, but it gives no information regarding the stiffness of the tooth surface. The model that we use to determine the compliance of the flank of the tooth, is based on the study of Marmo, Toraldo, A. Rosati and L. Rosati that gives a numerical solution to the computation of the contact pressure. The first step that must be performed consists in the generation of the compliance matrix of the tooth surface. This matrix does not depend on the angular position of the tooth, and therefore can be performed only once, at the start of the script. For this task a specific matrix was developed for the case of external gears; since there is no difference in the case of our surface, this function can perform the task without any modification. The function discretizes the surface of the tooth into triangles, that will be the discrete areas on which the pressures will be computed. As an output it will generate the compliance matrix $[uzz]$, the area, and the position of all the triangles and nodes the compose the tooth flank.

Load sharing factor

The load sharing factor describes what percentage of the total force transmitted between the gears is transmitted by each couple of teeth in contact. The output is an array with the fraction of the total force that is applied to each tooth. To compute the load sharing factor the first step is to understand what teeth are in contact. The distance between the selected teeth is calculated, as well as the coordinate and node at which the profiles are in contact. The teeth assumed in contact in this step are the theoretical ones, that would be in contact even if there was no tooth deformation and the static transmission error was zero. For the first attempt, on these theoretical couples of teeth in contact, a unit load is assumed. In the cycles after, the actual load that was computed in the previous step will be used. This load will generate a displacement of the tooth due to shear and bending stresses and to tooth base deflection, the couple of teeth that deforms less will have a higher share of the load on it.

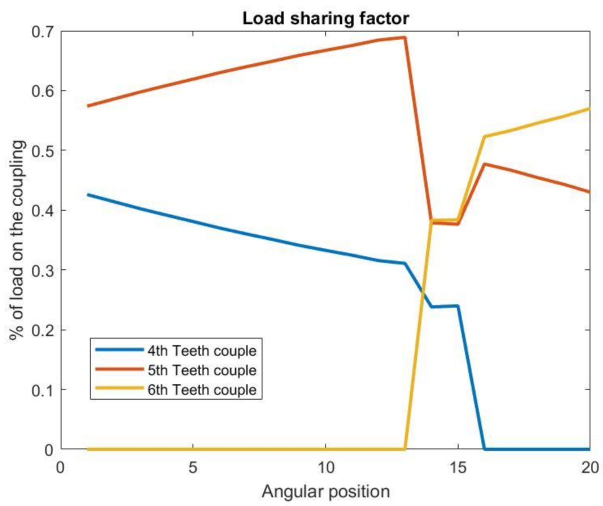

Figure 22"Load sharing factor"

$$Y_j = \sum Y_k \quad \forall\, k \neq j$$

$$LSF_j = Y_j / Y_{TOT}$$

As is shown in the formulas, the load sharing factor on the j^{th} couple of teeth is equal to the deformation on all the other couples in contact, divided by the sum of all the deformations on all the couples. The final output of the function is the array LSF, that contains all the percentages of load that are discharged on each teeth couple. These values can be represented for all the twenty angular positions of the profiles. As can be seen in the picture, the teeth coupling number four goes out of contact around the 16^{th} position, whereas tooth number six, goes into contact at the 14^{th} angular position. As the load on the 4^{th} teeth coupling progressively decreases, the load on the 5^{th} increases. It can also be seen that if there was a 21^{st} angular position of the teeth, it would have the same values as the 1^{st}, only shifted by one tooth. This happens because the 21^{st} angular position is exactly equal to the 1^{st}.

Teeth deformation due to loading

Once the first attempt at determining the load on each tooth in contact has been made, it is possible to start the cycle that iteratively tries to determine the actual static equilibrium for the gear coupling. Once the position of the teeth profiles at the equilibrium has been determined it will be possible to compute the static transmission error.

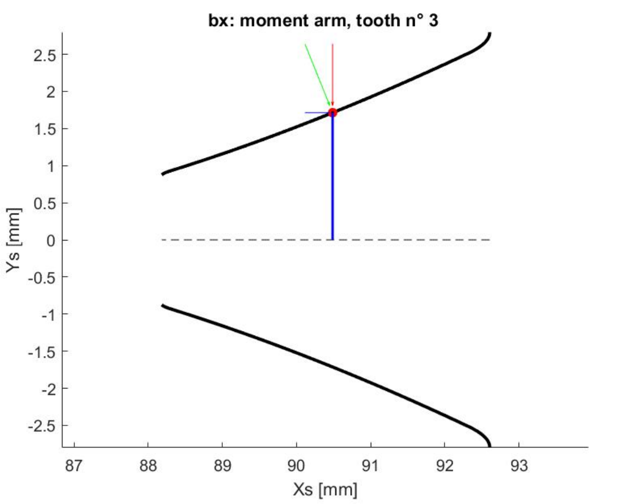

Figure 23 "Direction of the forces on the tooth"

As a first step of the cycle, the deformation of the teeth given the loading determined in the previous step is computed. This is subdivided into two types of deformation, the first one is the deformation due to bending and shear forces. This is computed with the stiffness matrix that has been derived at the beginning of the script, and that the was correctly modified for the ring gear. The other element necessary to determine the deflection of the tooth is the force amplitude and direction. The amplitude was estimated in the first attempt load sharing factor calculation, the direction, called μ_{eff} is computed in its respective function and in the case of internal gears, it must be rotated by 180 degrees, since it does not understand what side of the flank is in contact. In the figure on the side, it is possible to see that the force acting on the side of the internal tooth, the arrow in green, is correctly positioned and divided into the two main axial directions.

Since the force direction and amplitude are computed, as well as the stiffness matrix is correctly constrained and calculated, it is possible to compute the displacement of the teeth in contact for the ring gear.

As it is shown in the figure, the tooth is correctly constrained for the highest value on the x axis, that represents the root of the tooth on the annulus, this validated the correct definition of the constraints for the stiffness matrix that was previously computed.

The second step to evaluate the deformation of the teeth due to the loading force, is the tooth foundation deformation. This formula, developed by Sainsot and Velex, that is currently used in the script, has been validated only for externally toothed gears. Since the elaboration of a new formula is beyond the scope of this thesis, it has been decided to compute the value of the foundation compliance for the internal gear, as if it was an equivalent external one. After this equivalent value has been computed it is corrected, stiffening it by 20%.

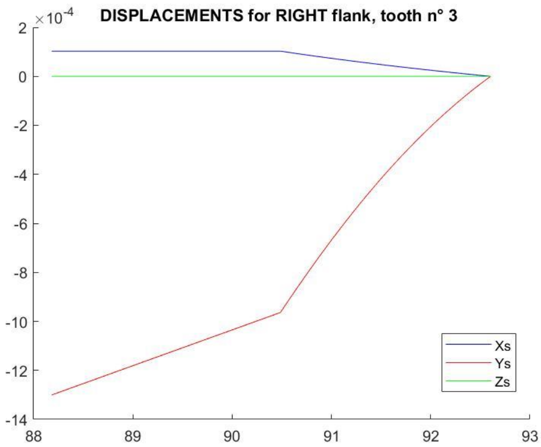

Figure 24 "Displacements of the tooth based on the node"

The values for the deformation that have been obtained in these steps will be used to shift the profiles of the teeth that are in contact, generating a gap between the profiles. This gap is called the static transmission error (STE), although, since this is only the first guess value of this error the equilibrium position still has not been reached.

Evaluation of non-contact couples

Once the profiles have been deformed it is possible to evaluate another occurrence, the contact between teeth couple that should not theoretically in contact. Due to the deformation of the profiles, especially under heavy loads, it is possible that a couple of teeth that geometrically is not in contact reaches contact. To analyse if this is the case, an opportune function has been developed, it uses many of the functions that have already been described in the previous steps, therefore no further modification is necessary to make it work also for the planet/ring coupling. The basic principle that it uses to check for the return in contact of any other couple of teeth, is that the gap angle between the profiles that are not in contact is smaller than the maximum STE of the loaded couples. This check is going to be performed at every cycle of for the calculation of the equilibrium condition.

Independently to the occurrence of this additional load couples, the script must recalculate the load sharing factor, now with the actual displacements of the teeth. It is achieved by comparing the torsional stiffnesses of each couple of teeth, calculated in $[N * mm/rad]$. The principle is that the higher the stiffness the more load will discharge on that coupling. It is possible that in the recalculation some coefficient might be negative. Since negative coefficients are impossible, because they would mean that a negative force is being transmitted between the gears, a recalculation is necessary. In the recalculation the couple of teeth with a negative load sharing factor will be excluded. Once this final load sharing factor is determined, they cycle to determine the static equilibrium can restart from the function the displaces the profiles.

Final equilibrium position

After a given number of cycles, the coupling should converge to the static equilibrium position, and the load sharing factor is set. For the given equilibrium condition, it is possible to find the node of the profile that is closest to the actual contact position between the teeth coupling. In the case of the results that have been obtained, it was iterated for twelve times.

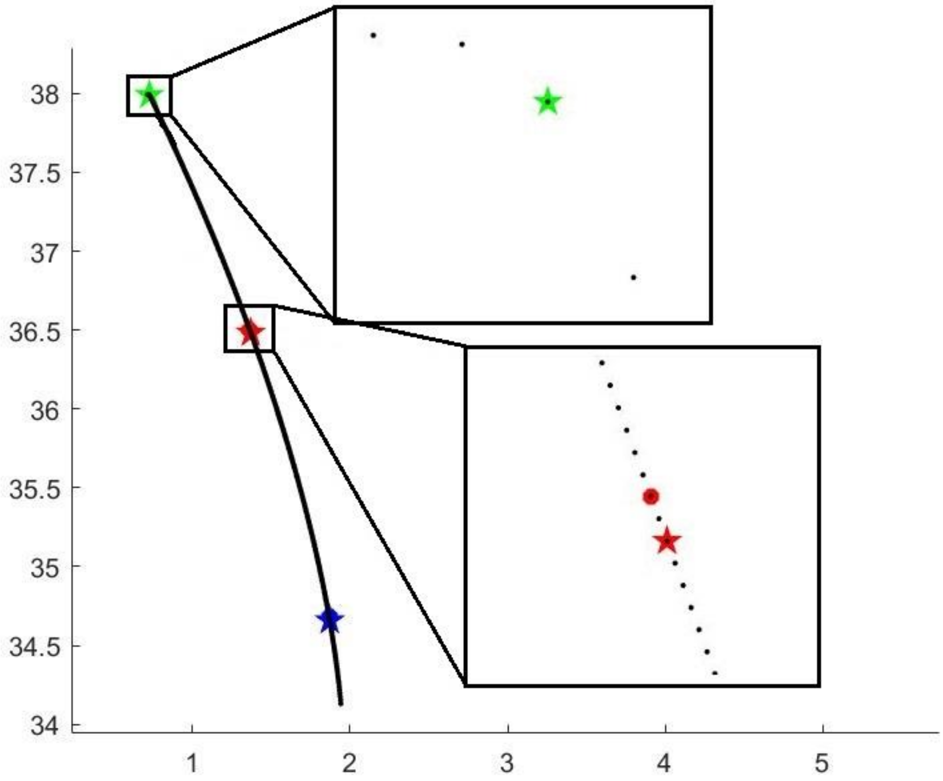

Figure 25 "Contact points on the flank of the planet gear"

As it is possible to see in the figure above, the gear coupling reaches the static equilibrium with three couples in contact. The tip contact point would not theoretically be in contact, but due to the deformation of the teeth, some of the load will be discharged also by his coupling. For this reason, only the green star is present, because the dot is the first contact point determined without any load being applied. In the other hand the star indicates the final equilibrium contact point. For the red and blue couplings, the circular point is present, because they were determined to be in contact even if there was no displacement of the teeth under loading. As it is possible to see for the red coupling, in the case of the pinion, the difference

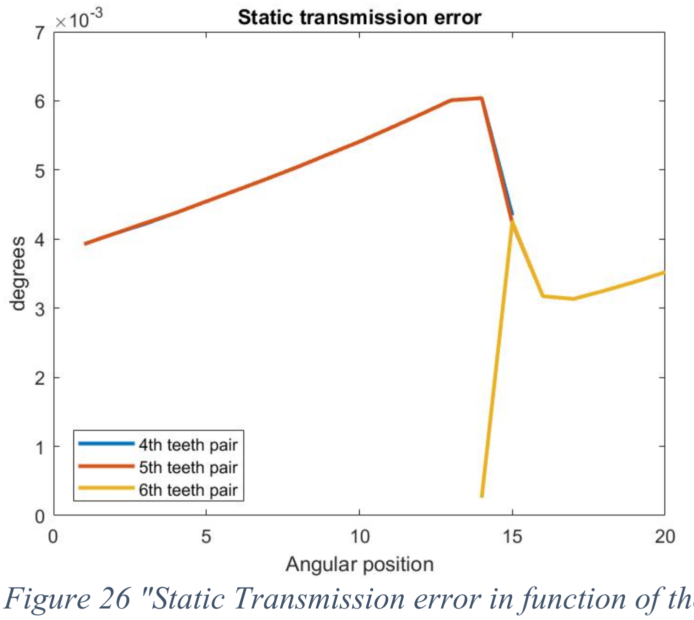

Figure 26 "Static Transmission error in function of the angular position" between the theoretical contact point, and the actual contact under loading, is of two nodes, since the red circle is two nodes under the red star.

As a last step the static transmission error is computed and saved in the structure that will end up in the final output of the script. The calculation of the STE uses the function that computes the angle between teeth profile, in this case in will be the angular distance of the profiles at the equilibrium condition. The value will be given in degrees for all the contact positions that have been studied, the same way as it was for the load sharing factor. If the tooth coupling is not in contact, then it will not be computed.

Contact pressures

Once the teeth profiles that are loaded are in the equilibrium position it is possible to estimate the contact pressures that arise from the loading condition to which they undergo. To achieve it, the dedicated function, uses a method developed in [4]. This method allows for the fast evaluation of the contact pressures between different types of surfaces. It is an algorithmic approach that solves a linear system of equations and performs an iterative process until the integral of the pressures over the respective contact areas are equal to the force exchanged between the teeth.

Contact plane

The first function generates the surface that is tangential to the contact point. To achieve this result, it takes the contact node and profile of the planet gear that have been calculated at the static equilibrium. From this data, it is possible to mathematically calculate the plane that is tangent to the contact node. The contact surface is a part of this plane limited both in the x and y directions. The size of the boundaries of the surface depends on the y axis on the tooth width, and on the x axis, on the estimated size of the contact area between the surfaces. The size of the contact area is estimated by computing the contact pressure and width with the Hertzian theory. The function also determines the boundaries of the tooth, and saves them, in this way the distance between the tooth profile and the tooth is computed only inside of the boundary. If the boundaries are not defined correctly, then the script will not compute these values.

To ease the next step in the process, instead of saving the contact surface position and angle with respect to the planet gear, it is positioned in the x-y-z plane and centred in the origin. To correctly position the profile, a rotation matrix that achieves this task is computed and saved as the output of the function. This function did not require any modification, since the computation of the tangential plane to a surface, and the rotation of the profile do not vary from externally to internally toothed gears.

Distance from the contact plane

The methods that will be used requires the distance from the contact plane to the profile $h_a(x, y)$ to compute the pressures. In external gears the shape of the flank is fully convex with respect to the contact plane. In the case of internal gears, instead, it is mainly concave, and only the last part towards the tip is convex. This is due to the different conjugate action that occurs between an internally toothed gear and an externally toothed one. The function that computes the distance between the two profiles, handles one profile at a time. Since the process is the same for both gears it will be described only once.

The gear enters the script and its profile is rotated to have the contact point in the centre of the contact plane. From this position the distance between the contact plane and the profile of the tooth is computed and saved in the matrices $[zgg_1]$ and $[zgg_2]$.

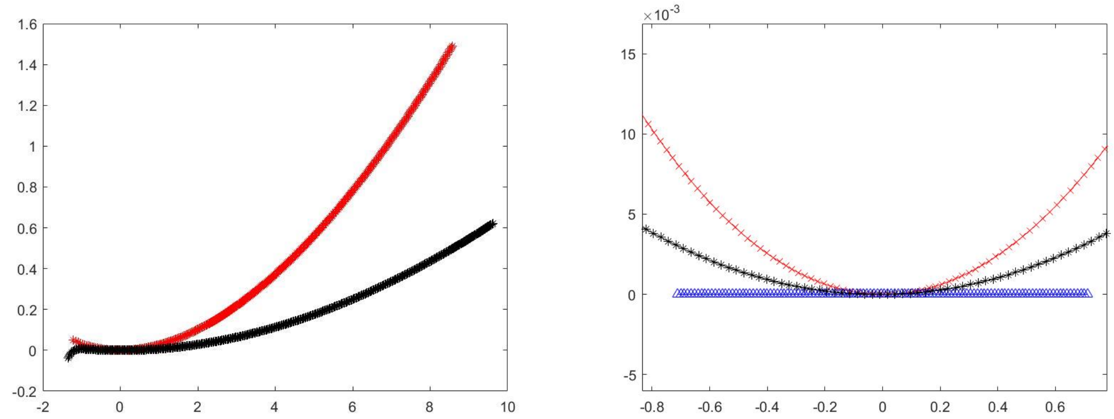

Figure 27 "Profiles of the gears in contact with tangent plane"

As can be seen in the figure above, the point of contact is centred in the origin of the plane. In the left figure in black, it is possible to distinguish the shape on the internal gear, with its peculiar tooth tip. This can be used as a reference to understand the relative position of the teeth. The main peculiarity of the internal gear is concavity of the tooth profile. For most of the flank the profile is concave, whereas in the externally toothed gears, like the red profile in figure, the profile is convex. If the tangential plane to the point of contact (0, 0) is considered, the distance from this plane of profile of the internal tooth brings it closer to the profile of the planet gear tooth. We will consider the effect of this phenomenon in the further steps, by ensuring that the negative sign for the values of this distance, do not give issues to the computation of the relative distances between the profiles.

Before entering the pressure calculation function this distance values must be manipulated as to have the correct definition to perform the next operation, this means adding the null values in the points that were not computed due to being outside of the contact plane surface. Each array of the matrices zgg_1 and zgg_2 will be shifted as to having the closet point to the surface with a value of zero. Once these arrays are correctly modified, they are saved in the matrices h_a and h_b.

Another variable that is initialized before entering the iteration for the pressures is Δz, that describes how much penetration occurs between the profiles. To compute this value, it is assumed that the profile of the pinion is rotated by a fist trial angle $d\vartheta$, from this angle the displacement of the profile is computed, and the values are saved in an array that enters the pressure calculation function.

Pressure iteration

The calculation of the contact pressures is based on a model developed to specifically compute the contact pressures on surfaces.

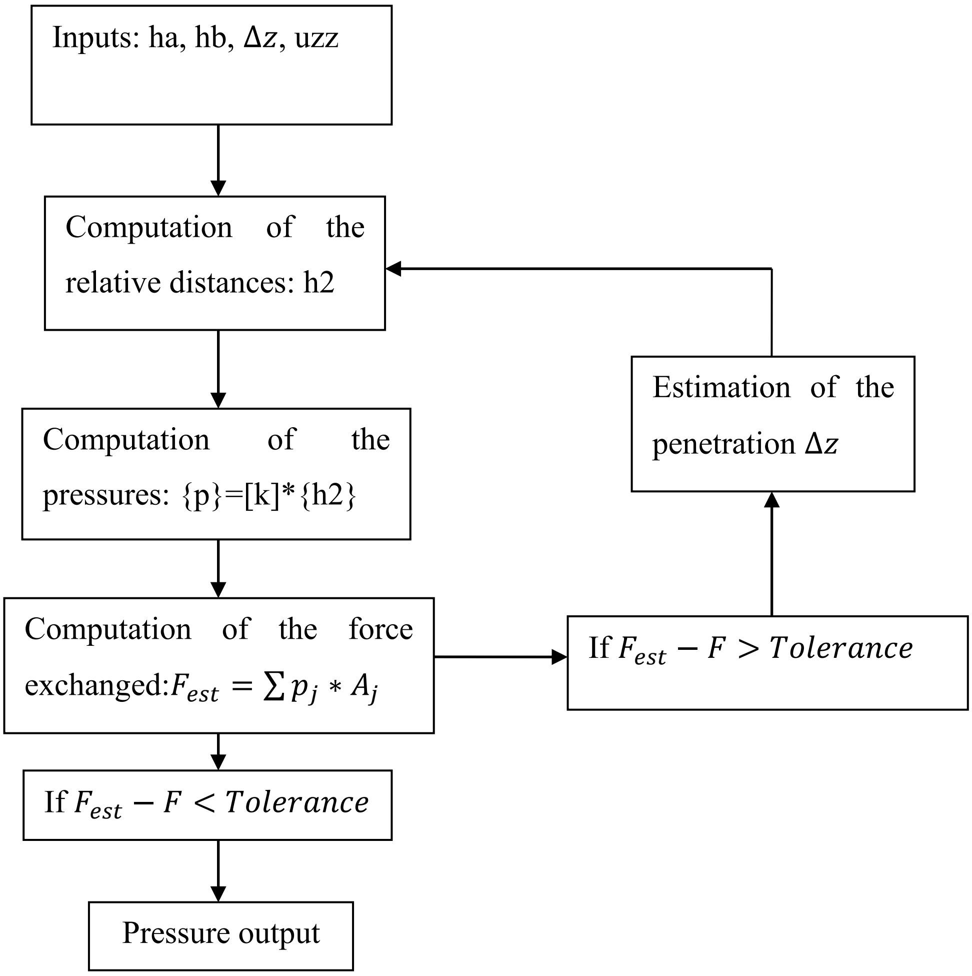

For the given tooth couple th from 1 to the number of possible teeth couples, the corresponding array of h_a and h_b enters the function, along with the corresponding array of the delta z matrix. As the function enters the displacement of the profiles is computed and saved in the array h_2, the zero values are removed from this array and stored in the subsequent h_1 array. For the first computation of the pressure, the first guess value is used in the formula:

$$\{h_2\} = \{\Delta z\} - \{h_a\} + \{h_b\}$$

And it is possible to see that even if the array of h_b has negative values, this causes no issues. Then the pressures are computed by solving the linear system of equations:

$$\{p_{mar}\} = [uzz]^{-1} * \{h_1\}$$

$[uzz]$ is the correctly sized, for the array $\{h_1\}$, compliance matrix of the tooth, that was previously computed. The inverse of the compliance matrix is the stiffness matrix, that multiplied by the displacement gives the forces, that, divided by the unit value of area give the pressure. Once the pressure has been computed it is summated on the area of contact with the formula:

$$F_j = \frac{1}{3}\sum_{a=1}^{n} A_j * (p_j(\rho_1^a) + p_j(\rho_2^a) + p_j(\rho_3^a))$$

That gives the value of the force exchanged in the triangle j, F_j. A_j is the area of the triangle, and it was computed with the compliance matrix. By adding F_j on the whole contact area of the tooth, the total force exchanged is computed. This force is then compared with the actual forced exchanged in the coupling, that was determined with the load sharing factor previously derived. If the value is within a certain tolerance the iteration will stop and exit and save the array of the contact pressures for that coupling and start again for the next coupling that is under load. When all the couples of teeth that exchange a force have been considered all the pressure values for that angular position are saved in their own array, and the script will start the cycle for the next angular position. As it can be seen in the figure, the contact pressures can be plotted as a function of the node. This type of visualization of the pressures describes the behaviour of the pressure both on the x and y axis since the nodes are coherently distributed along the face width of the tooth. The

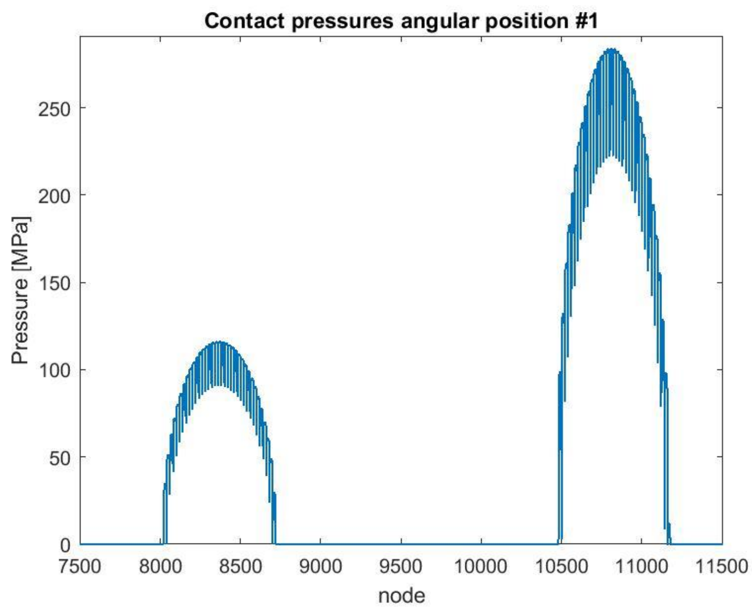

Figure 28 "Contact pressures in the first angular position" local maximum and minimums are caused by the varying pressures along the face of the tooth, the higher values are at the centre, and they gradually decrease towards the side.

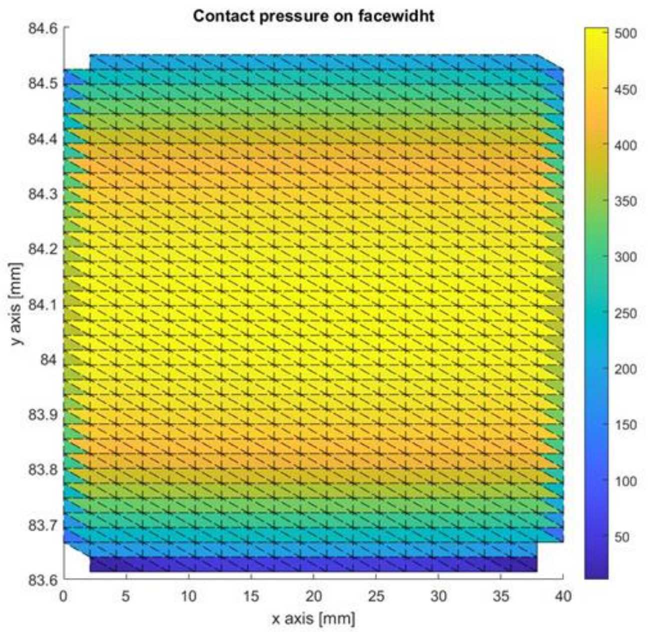

Figure 29 "Pressures on the face width of the tooth"

To see this phenomenon, it is possible to represent the pressures also as a function of x and y. In this representation the triangles of the discretization on which the pressures have been computed are represented, and the pressure is no longer shown as the value on the node, but as the average of the nodes that compose the triangle. It can be noted that the pressure is higher at the centre of the face width, and decreases when moving from the centre both in longitudinal and transversal direction, as it would be expected.

Results

The case that we will study has the following characteristics.

Parameter	Value	Unit of measurement
z_{sun}	24	-
z_{planet}	33	-
z_{ring}	90	-
z_{shaper}	30	-
Rotational speed (Planet)	1000	rpm
Number of planets	3	-
Tooth modulus	5	mm
Pressure angle	20	°
Tooth face width	40	mm
Gear body face width	40	mm
Helix angle	0	°
Gear Material	15CrNi6	
Shift coefficient	0	-
Addendum	1	-
Dedendum	1.25	-
Ring gear backlash	200	μm

For this case the analysis will be performed with 200Nm, 800Nm, 1600Nm and 4000Nm. The respective safety factor against bending fatigue (ISO 6336-3) are shown in the table below

Torque	200Nm	800Nm	1600Nm	4000Nm
Ring gear S.F.	31.5	15.7	9.6	4.4
Planet gear S.F.	28.7	14.3	8.7	4

As it is possible to see, the loading condition never exceeds the safety factor to bending by a good margin, this ensures that the results that have been obtained are not under very heavy loading. This prevents computational mistakes that might occur in the case of heavy loading conditions.

Influence of torque on the load sharing factor

The main effect that influences the load sharing factor with the increase of torque, is the number of teeth couple that are in contact. For higher loads the deformation of the teeth is higher, and this causes the load to be spread on a higher number of teeth couples. As it can be seen in the figure, we have considered the two most extreme cases of loading. In the case of a light load of 200 Nm, the contact of the 6th teeth couple starts only at the 14th angular position, whereas for the 4000 Nm case, is already starts at the 8th angular position. When the load is not spread out on more than two different couples of teeth, the load sharing factor is practically the same since the stiffness for the given angular position is the same.

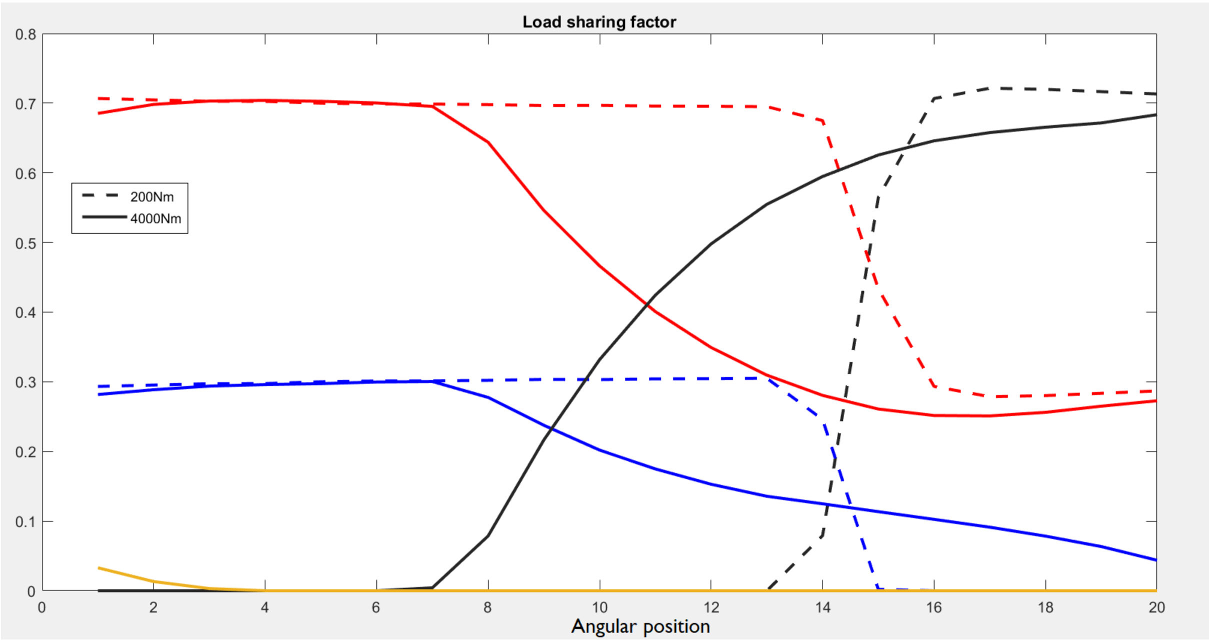

Figure 30 "Load sharing factor as function of torque and angular position"

To show how the load progressively evolves with increasing loads only a couple of teeth has been chosen, since it would be too confusing to plot all the teeth couples for all four of the cases that have been considered. It is possible to see that with the growing load, the angular position of first contact for the 6th teeth couple come earlier, causing the load on the 5th couple to decrease. In the case of the 4000 Nm load, it can also be noted that in the first angular position, for the first 4 positions the share of the load is lower since the 3rd couple of teeth is still contact. This results appear to be accurate, and the effect of the growing load on it follows the behaviour that would be expected.

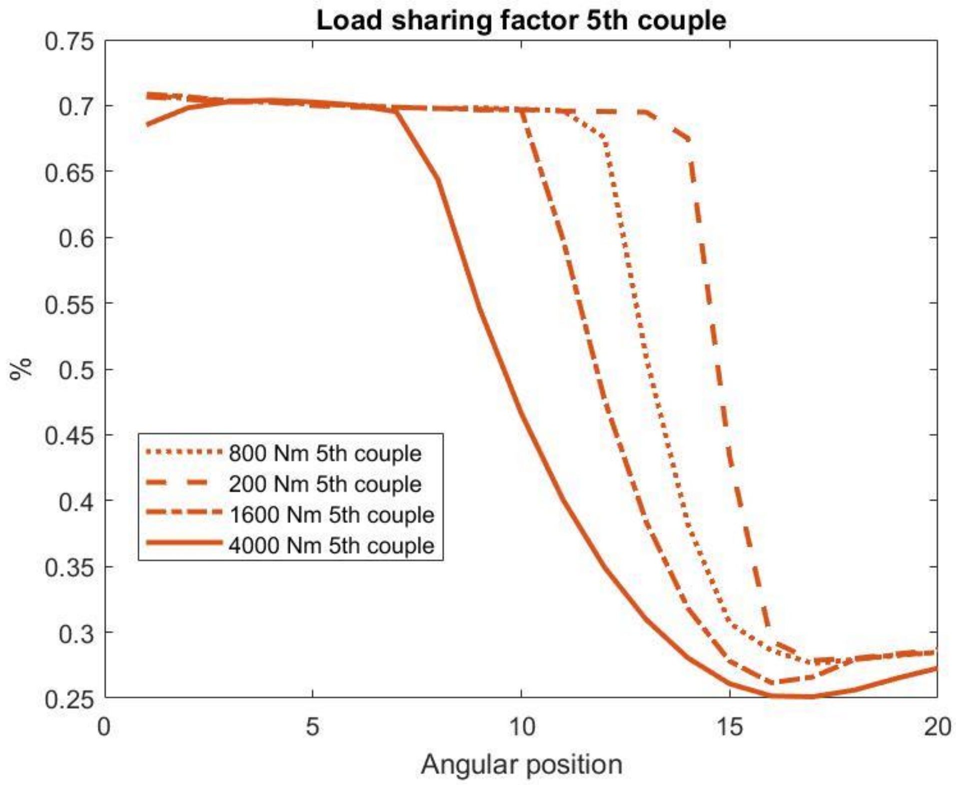

Figure 31 "Load sharing factor of the 5th teeth coupling"

Static transmission error

With growing torques, the teeth are subjected to growing forces, and thus to greater displacement with respect to the theoretical meshing. This leads to a greater value of the static transmission error. Moreover, the peak of highest transmission error is shifted to lower points in the loop of angular position. This is again caused by the earlier contact of the 6^{th} contact couple, that increases the stiffness of the teeth couple.

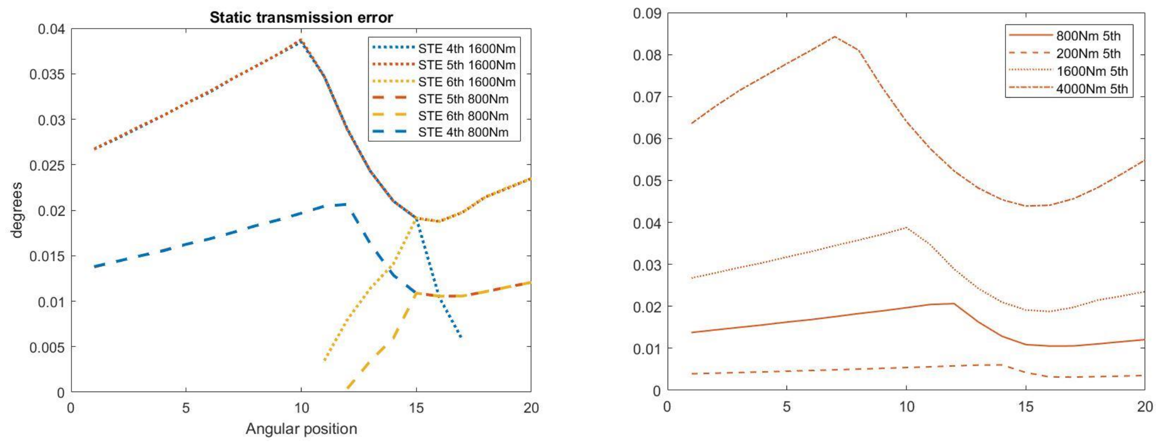

Figure 32 "Static transmission error, effects of load and angular position"

The checks that have been performed for the values of the load sharing factor, and static transmission error, are not indicative of the actual behaviour of the gear coupling, since, as we mentioned before, the computation of the tooth root deformation is not accurate. The check on the values of this parameters is based on a tooth root strength that was estimated, and they indicate that if the computation of this strength is accurate, then the script can produce results also for an internally toothed gear that meshes with an external one.

Contact pressures

Once the reliability of the script that determines the loading and the contact position of the teeth profile it is possible to check the values of the contact pressures. In the first angular position, for all the cases, except the 4000 Nm one, there are two points of contact, and it is possible to compare how the growth of the contact force influences the pressure. With growing forces, the pressures increase, as it is logical. Even though it looks like the contact area remains the same, this is not the case. On the x-axis there is the node, this means that it does not show the length of the contact area along the profile, but the number on nodes on which there is deformation. These nodes are the product of the discretization of the tooth face and are spaced based on the contact area computed with the Hertz formula for the contact surface. This means that with growing forces, the contact area increases, and therefore the nodes are more spread out. What can be deduced from this plot is that the model that computes the pressures is consistent with respect to the value of the contact area determined by Hertz. The main difference is in the shifting of the contact area, due to the growing deformation of the teeth. With higher loads the contact point at the equilibrium moves towards the internal gear, causing a shift in the peaks, and of the nodes on which there is deformation of the profiles.

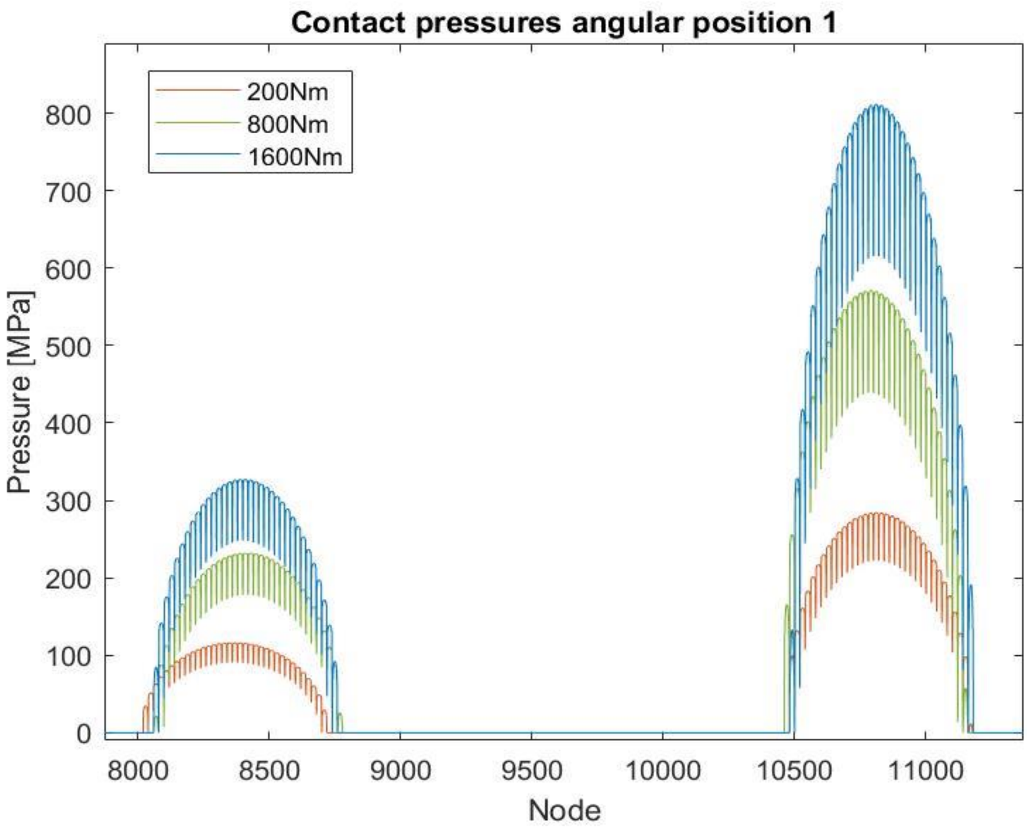

Figure 33 "Contact pressures on the first angular position"

In the following figures the pressure is plotted on the face of the tooth, in combination with the tooth meshing, this means that the pressure on each node has been averaged on the triangle on which it belongs, then they are painted on the graph.

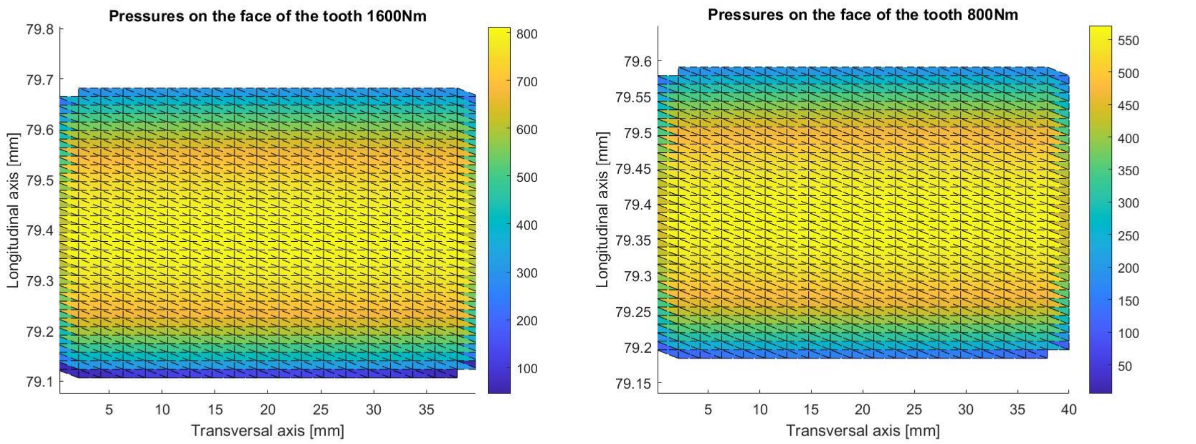

Figure 34 "Contact pressures on the face of the tooth, comparison between different torques"

As it is possible to see in the figures, the contact area is smaller on the face of the tooth that is subjected to a lower force. If in the case of 1600 Nm the contact area goes from around 79.1

mm to 79.7 mm, in the case where it is loaded with 800 Nm, the contact surface goes from 79.2 mm to 79.6 mm.

The pressures were also computed with the Hertz method for deriving contact pressures in gears with the formula:

$$p_{Hertz} = \sqrt{\frac{E_{red}}{2\pi} * \frac{F_n}{b * \sin(\alpha)} * \frac{r_1 + r_2}{r_1 r_2}}$$

In the table below are reported the values of the pressures determined with the Hertz formula compared with the one computed with the iterative method.

Torque	200 Nm	800 Nm	1600 Nm
p_{Hertz}	394.3 MPa	788.6 MPa	1115.2 MPa
p_{iter}	283.8 MPa	564.3 MPa	805.6 MPa

The pressures determined with the Hertz method are lower than the one computed by the script, but they are consistently so, since instead of considering all the load on just one tooth, the load is spread out on two couples of teeth. It is possible to compute the pressure with the Hertz method on each couple of teeth by multiplying it by the square root of the load sharing factor. The pressure computed with the Hertz method on the i-th couple of teeth is:

$$p_{Hertz,i} = \sqrt{\frac{E_{red}}{2\pi} * \frac{F_{n,i}}{b * \sin(\alpha)} * \frac{r_1 + r_2}{r_1 r_2}}$$

With $F_{n,i}$, the normal load on the i-th couple:

$$F_{n,i} = F_n * LSF_i$$

Substituting in the previous equation:

$$p_{Hertz,i} = \sqrt{\frac{E_{red}}{2\pi} * \frac{F_n * LSF_i}{b * \sin(\alpha)} * \frac{r_1 + r_2}{r_1 r_2}} = p_{Hertz} * \sqrt{LSF_i}$$

It is possible then to compute the pressure, even if not with total accuracy since the contact point is not on the pitch line of the teeth.

Torque	200Nm 4th	200Nm 5th	800Nm 4th	800Nm 5th	1600Nm 4th	1600Nm 5th
LSF	29.24%	70.76%	29.26%	70.74%	29.13%	70.87%
$p_{Hertz,i}$	213.2 MPa	331.7 MPa	426.6 MPa	663.27 MPa	601.9 MPa	938.8 MPa
p_{iter}	115.8 MPa	283.8 MPa	230 MPa	564.3 MPa	322.1 MPa	805.6 MPa

A difference between the two values remains, and it should be noted that curvature of the tooth profiles is computed at the pitch radius of the gears, this means they we have corrected only for the normal load to the tooth. To accurately compare with the pressure values obtained with the Hertzian formula it is necessary to find an angular position that is close to the pitch circle, around the radial value of 82.5mm on the planet gear.

As it is possible to see from the table below in this area the computed values are very close.

Torque	200 Nm	Radial position
p_{Hertz}	323.8 MPa	82.5 mm
p_{iter}	334.6 MPa	82.67 mm

Pressures on the tip of the planet gear

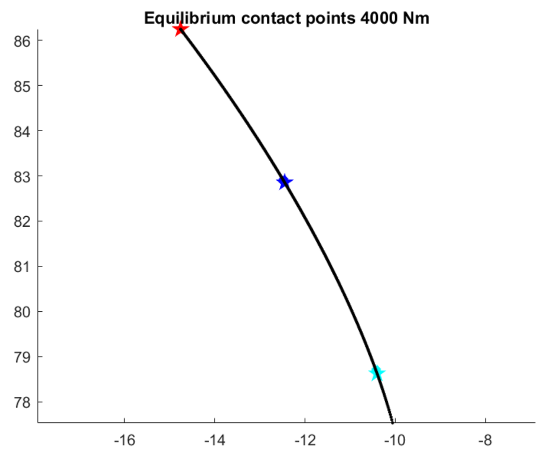

Figure 36 "Contact pressures under heavy loading"

Having cleared the fact that the script is able to compute the contact pressures when the teeth profiles are in contact on one position of the flank that is continuously defined on the theoretical surface area. If the teeth are in contact next to the tip of the planet gear, this condition is no longer satisfied. When the torque on the planet gear is equal to 4000 Nm, in the first angular position there is a return into contact of the 3rd teeth couple. This contact point is on the tip of the planet gear and is shown in red in the figure. The addition of this contact point modifies the load sharing factor, as it has already been seen. Therefore, a part of the load is discharged by the tip of the planet gear. This condition means that the distance between the profile of the planet gear flank and the theoretical contact plane can be computed only for half of it. In the normal computations, the discretization of the contact plane by means of triangles uses 20 steps in the transversal axis, and 120 steps on the longitudinal axis. If the script computes the pressures for this condition, it does not have enough points that experience actual deformation, and results in the error "no node is surrounded by nodes to form a triangle". To achieve the computation of the pressures in this case there are two possible paths. Either the estimated contact area is modified, or the discretization on the longitudinal axis of the tooth is made finer.

By increasing the value of the discretization "ny" to 1000, the script returns the values of the contact pressure. This step increases the computational time both for the compliance matrix against the contact forces, and the computation of the pressures. Resulting in an excessive time elapsed. The pressure that is computed by adopting a finer meshing of the tooth face results in values of the pressure exceeding 6000 MPa, beyond the surface pressure strength of any type of material that is used in the manufacturing of gears. For these reasons, assuming that the equilibrium position is computed correctly, a heavy loading of this gears would lead to a condition of high pressures, that should be avoided. Therefore, it is not necessary to increase the discretization of the tooth flank. If there are not sufficient nodes, with the discretization of ny in twenty segments, it means that the contact pressures are way too high. We will not perform the same analysis by reducing the estimated surface area of contact, because this would impede the correct computation of the pressures for the other loading conditions.

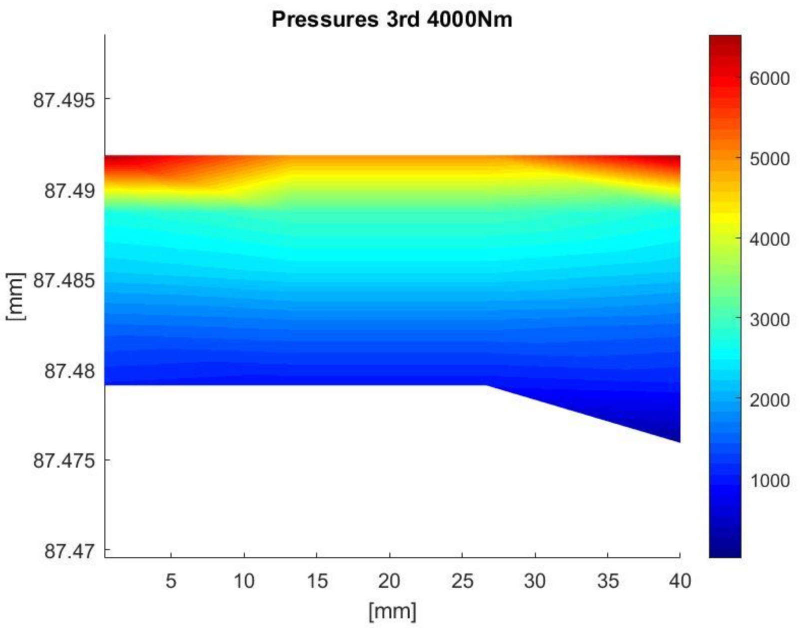

Figure 37 "Contact pressures on the tip of the planet gear"

Other loading conditions

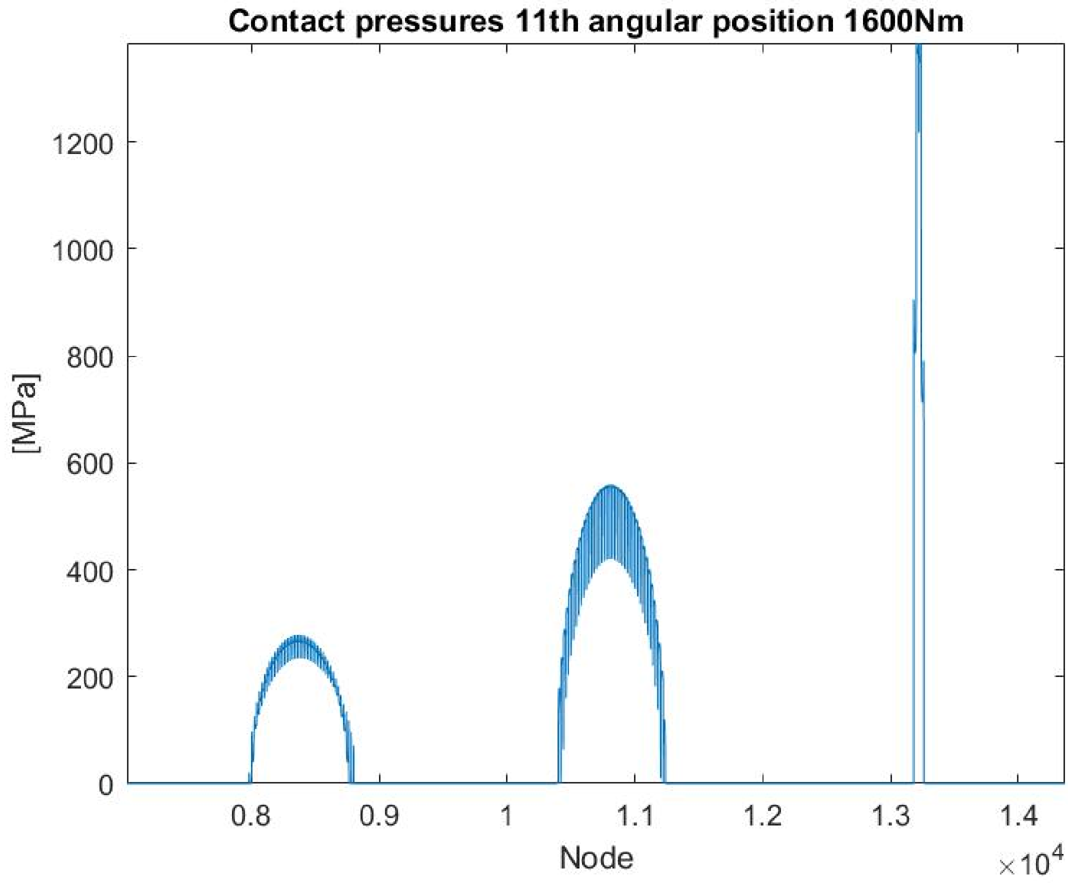

Figure 38 "Contact pressures 11th angular position"

In some cases, there are three teeth couplings in contact, in some of those cases, a pressure peak on one of the couplings can be observed. This is the case for the 11th angular position when the pinion is loaded with 1600 Nm. This leads to a spike in pressures towards the fillet of the planet gear. This means that the tip of the internal gear, when penetrating this part of the planet, can cause significant overpressures. Another peculiarity lays in the concavity of the pressures. To understand what is happening it is useful to see the pressures plotted on the face of the tooth.

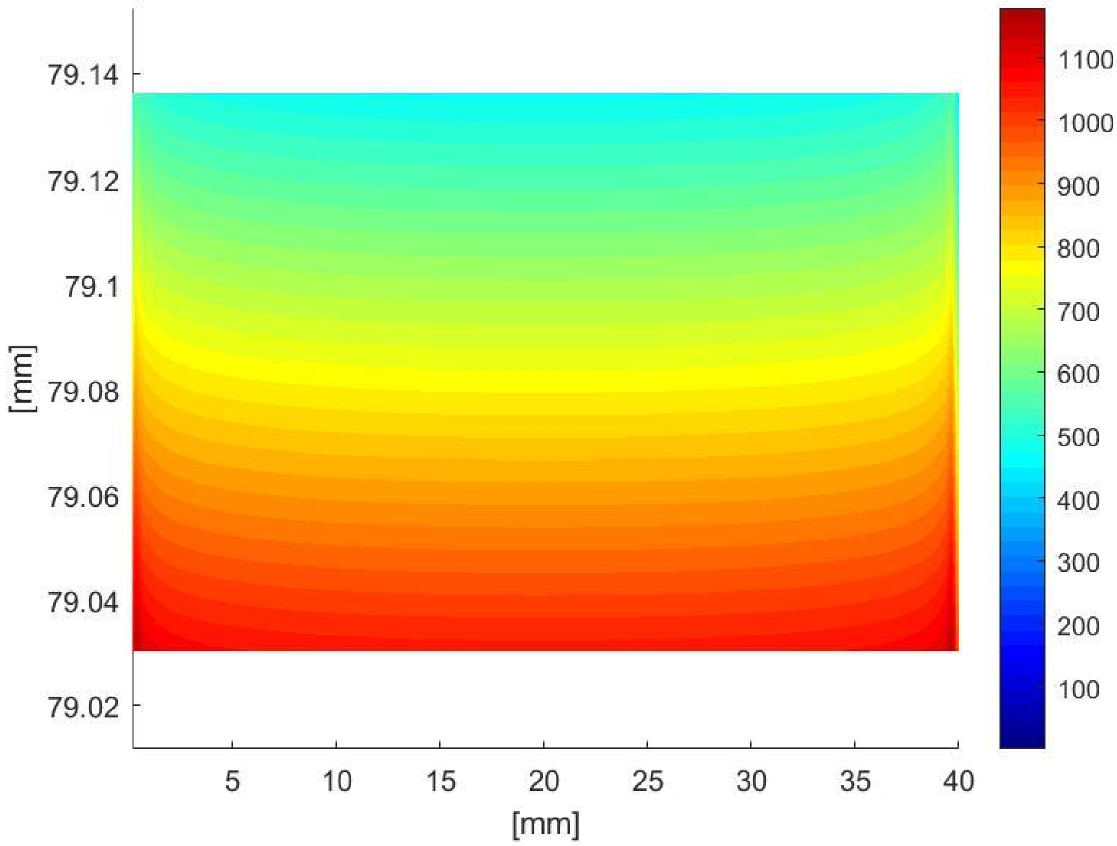

Figure 39 "Angular position 11, pressures on the face of the tooth"

As it can be seen in the picture, the pressures are quite high, and their values are highest on the lower part. This might be due to the peculiar shape of the tip of the ring gear, that changes concavity in that region. Therefore, the points that are higher on the y-axis see the part of the tooth that is concave, whereas the points on the lower part are in contact with the convex part of the tooth profile. The contact pressures between two profiles with the same curvature will be lower than the one where they have opposite curvatures, and for this reason the pressures are higher on the lower part of the tooth. To understand better this phenomenon the profiles that generate this pressure distribution are plotted in figure 38, together with the contact area, in orange, on which the gap function is computed.

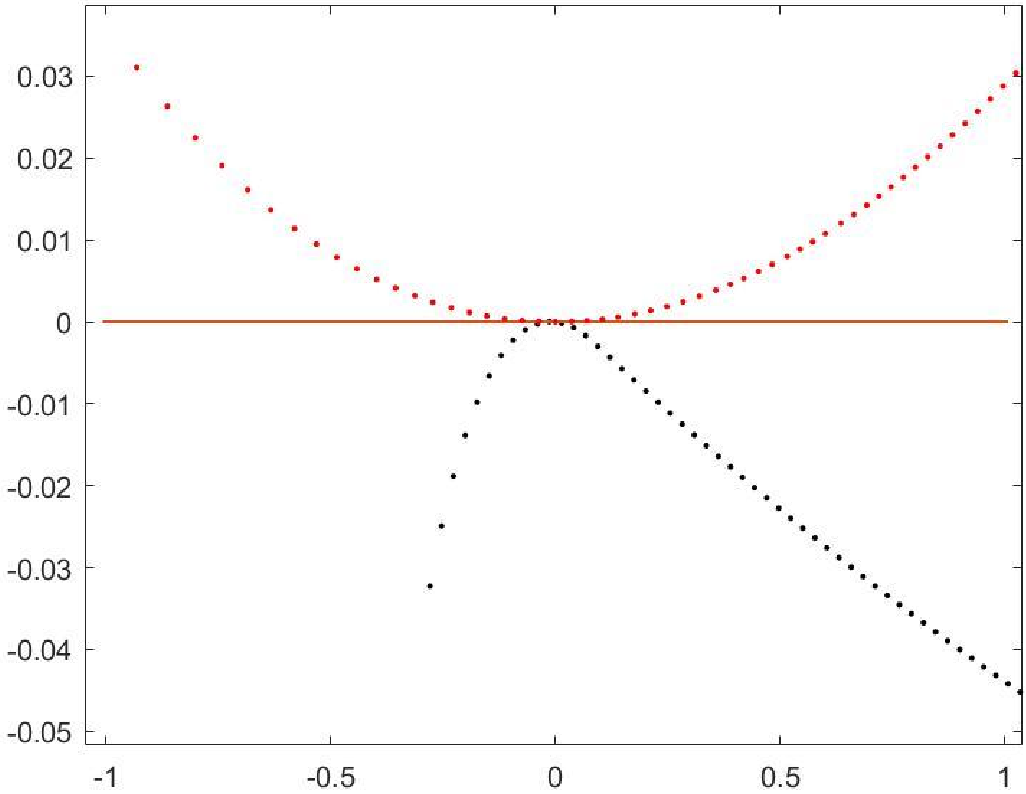

Figure 40 "Tooth profiles angual position 11"

Further developments

Given that the modifications performed show the possibility of applying this model for the computation of the static transmission error, and contact pressures in the meshing of an internal and external gear, it is possible to further improve the script. The first step is to validate another analytical formula for the computation of the tooth deflection cause by the gear body since the current formula has been validated only for externally toothed gears.

The other step that must be achieved to completely understand the behaviour of the whole planetary gearset is to allow for the meshing of the gear in multiple points. These considerations are relevant because the ring gear does not mesh with only one planet, but with multiple, at different positions on its circumference. The planet meshes both with the ring and the sun gear, and the sun, just like the ring, meshes with all the planets. When all these developments will be achieved it will be possible to add also the dynamic effects that affect this type of transmission.

Conclusions

To recapitulate, the script, starting from the correctly dimensioned and generated ring and planet gear, of an epicyclic transmission computes the static transmission error, and contract pressures for this mating couple in twenty different angular positions. The pinion, that in this case is the planet gear, receives different input torques ranging from 200 to 4000 Nm. The results that have been obtained are coherent with what can be theoretically determined, and the script can reliably perform this type of computation for any type of correctly sized coupling of this type. In case of heavy loading the script can compute the static transmission error. Although when computing the contact pressures, if the standard discretization of the tooth flank is used, it is unable to perform the task. This issue can be addressed by increasing the discretization, but, due to the high loading, the values that will be obtained cannot be assumed to be accurate. Therefore, with the standard discretization, if no pressure is computed, then it can be assumed that the contact pressures are too high, and either the load must be reduced, or the correct profile modification of the tooth applied.

References

[1] ISO 6336-1:2019

[2] ISO 6336-2:2019

[3] ISO 6336-3:2019

[4] **Marmo, F. Toraldo, F. Rosati, A. Rosati, L.** *Numerical solution of smooth and rough contact problems*, 2017.

[5] **Vullo V.** *Gears, Volume 1: Geometric and Kinematic Design*, 2020 (Springer).

[6] **Müller H. W.** *Epicyclic drivetrain,* 1971 (Springer-Verlag) (Berlin-Heidelberg).

[7] **Sainsot P., Velex P, Duverger, O.** *Contribution of Gear Body to Tooth Deflections—A New Bidimensional Analytical Formula,* 2004 ASME